MSUCL-219
MSUNC-187
October 1976

Rotational and Intrinsic Structure of ^{182}W from the $(\alpha,2n\gamma)$ Reaction and Decay of ^{182m}Re*

B. D. Jeltema, F. M. Bernthal, T. L. Khoo,

and C. L. Dors

Departments of Chemistry and Physics and Cyclotron Laboratory

Michigan State University

East Lansing, Michigan 48824

NUCLEAR REACTIONS ^{180}Hf(α,2n)^{182}W, E_α = 26 MeV; measured E_γ, $I_\gamma(\theta)$, I_γ vs. E_α, $\alpha\gamma$-delay, $\gamma\gamma$-coinc. ^{182}W deduced levels I, π, γ-branching, K. Ge(Li) detectors. Enriched target.

RADIOACTIVITY ^{182m}Re [from ^{181}Ta(α,3n); E_α = 41 MeV]; measured E_γ, I_γ, γ-γ coinc; deduced logft. ^{182}W deduced levels, J, π. Natural target, Ge(Li) detectors.

*Research supported by the U. S. National Science Foundation and the U. S. Energy Research and Development Administration.

Abstract:

The ^{180}Hf(α,2$n\gamma$) reaction was used to populate states in ^{182}W. In-beam γ-ray spectroscopy experiments result in assignment of 59 levels to the ^{182}W level scheme. Eleven rotational bands are identified, and most of these are characterized. A previously-reported 1.4-μsec isomer is characterized as the $K^\pi = 10^+$ triplet coupling of $9/2^+[624]$ and $11/2^+[615]$ neutrons, the first seniority two $i_{13/2}$ configuration to be identified in the rare-earth deformed region. The strongly-coupled band built on this isomer apparently becomes *yrast* above spin 16. Data from EC-β^+ decay of 64-h ^{182m}Re were used to supplement the in-beam data.

1. INTRODUCTION

The level structure of ^{182}W has been investigated extensively in β-decay and transfer reaction studies, but except for a half-life measurement of an $I^{\pi} = 10^{+}$ isomeric state,[1] the high-spin structure is essentially unknown. The $(\alpha,2n)$ reaction can transfer twelve or more units of angular momentum, so that in-beam γ-ray spectroscopy is expected to yield significant new information on the band structure of intrinsic and collective states in ^{182}W.

We report in this paper the results of $(\alpha,2n\gamma)$ experiments on ^{182}W. This nucleus is of interest for several reasons. A number of high-Ω orbitals are expected to lie near the Fermi surface in ^{182}W. These should give rise to several low-lying, high-K two-quasiparticle states, some of which are expected to be isomeric, since decay to the ground state band would be K-forbidden. The earlier identified $I^{\pi} = 10^{+}$ isomer was characterized in this work. The high-spin results of this work further extend the systematics relevant to backbending phenomena in this region.[2,3] In addition, a detailed knowledge of the systematics of intrinsic and collective nuclear properties may yield a clearer understanding of hexadecapole deformations in this region.[4,5]

Analysis of the in-beam γ-ray data indicated that several errors existed in the proposed decay schemes for ^{182m}Re.[6,7] Therefore a limited reinvestigation of ^{182m}Re decay is also reported in this paper.

2. EXPERIMENTAL

A thin, self-supporting target of ^{180}Hf prepared at the Niels Bohr Institute[8] was bombarded with a 26-MeV α-particle beam to produce ^{182}W via the $(\alpha,2n)$ reaction. Singles γ-ray spectra to 1800 keV were obtained using a 10.4% efficient Ge(Li) detector with a resolution of 2.1 keV (FWHM) at 1333 keV. A representative spectrum is shown in Fig. 1. In addition, spectra to 600 keV were taken using a small high resolution Ge(Li) detector [650 eV FWHM at 122 keV]. A typical spectrum is shown in Fig. 2. Because of the complexity of the spectrum, excitation function and angular distribution measurements were carried out using the high resolution detector. Nearly all γ rays above 1000 keV seen in the $(\alpha,2n\gamma)$ experiments that could be assigned to ^{182}W were known from ^{182}Ta and ^{182m}Re decay, so that reliable multipolarity information was already available from conversion electron measurements[9,10] for the higher-energy transitions seen in both experiments.

A chip of ^{180}Hf metal supported by 65 μm Ta wire was used to collect γ-γ-t coincidence data. These data were taken at 180° geometry (each detector at 90° to the beam) using Ge(Li) detectors of 10.4% and 7.7% efficiency, and the coincidence events were stored serially on magnetic tape for later analysis. The time spectrum was gated appropriately to obtain both prompt and delayed coincidence information. Resolving time for the prompt coincidence gates was ≈50 ns. Contaminant γ rays resulting from the ^{180}Hf$(\alpha,3n)^{181}$W reaction and from the Ta wire were also present, but were easily

identified from previous studies of these reactions.[11,12] No contaminants from the $^{180}Hf(\alpha,n)^{183}W$ reaction were identified.

Half-life measurements were made using the thick target by correlating the γ rays from the target nuclei with the cyclotron beam bursts. Two half-life ranges were investigated. In the first experiment, delayed γ rays were observed between each beam burst (period ≈65 ns); in the second, a fast beam sweeper synchronized to the cyclotron RF was used so that only one beam burst in nine struck the target, extending the time between bursts to ≈0.6 μsec. The lifetime measurements revealed only the isomeric state located at 2230.6 keV, which decays into the ground band via transitions of 518.5 and 1086.5 keV. This isomer was earlier observed by Nordhagen, Diamond, and Stephens[1] to have a half-life of 1.4 μs, and will be discussed in more detail in the next section. The timing experiments make it possible to place an upper limit of 5 ns on the half-life of the other ^{182}W levels populated in-beam. The energies and intensities of γ rays which could be associated with levels of ^{182}W are given in Table I.

3. CONSTRUCTION OF THE ^{182}W LEVEL SCHEME

The level scheme for ^{182}W was deduced primarily from the coincidence data, and is shown in Figures 3 and 4. Much of the level structure below 2 MeV was known from decay work[6,7] although there are several errors in those decay schemes. A difficulty encountered in the analysis was the existence of a number of very low energy transitions. The conversion electrons associated with these transitions were measured by Harmatz *et al.*[9] and Ageev *et al.*[10] and the transitions are placed in the level scheme on the basis of energy sums and differences. In several cases these placements are also implied by our γ-γ coincidence data. In addition, some γ-rays too weak to be seen in-beam are known from ^{182m}Re decay. For completeness, all transitions associated with the γ-decay of excited states in ^{182}W are shown on the level scheme, but only the γ-rays actually seen in-beam are listed in Table I. Transitions placed on the basis of in-beam γ-γ coincidence data are indicated by dots underneath the arrows, and levels which were placed on the basis of uncertain coincidence evidence or energy sums and differences are dotted to indicate that the level assignment is tentative. All levels known from ^{182m}Re decay are also populated in-beam with the possible exception of the 1960.7-keV state. As will be discussed in Section IV, coincidence data for this state are difficult to obtain in the ^{182m}Re decay because of the intensity of γ-rays from the 1960.3-keV state. In-beam experimental conditions make this state even more difficult to identify from the $(\alpha,2n\gamma)$ data, so that it is impossible to confirm the existence of this state by coincidence measurements.

Spins and parities in the level scheme are based on the assignments from refs. 7 and 13. Where band structure can be extended beyond that seen in these references, spins are assigned based on the expected regular spin sequence of the band members. These assignments are in every case consistent with the angular distribution and excitation function data. However, a number of γ rays appear in the spectrum with intensities too low for reliable angular distribution measurements. Assignments which could not be supported by the angular distribution and excitation function data are indicated as tentative on the level scheme.

Most of the states in the level scheme could be assigned to the rotational bands in Figure 5. The large number of bands populated in the (α,2nγ) reaction results from an unusually high density of states near the ^{182}W *yrast* band. The bands were identified on the basis of the γ-ray decay patterns and the level energies shown in Figures 3 and 4.

A. Even Parity Bands

There were five even parity bands observed in this study. These are the ground, β- and γ-vibrational bands, a $K^{\pi} = 6^{+}$ two-quasi-proton band, and the $K^{\pi} = 10^{+}$ isomeric two-quasi-neutron band. A partial level-scheme of these bands including the prominent γ-ray transitions is given in Figure 6. The β- and γ-band assignments are consistent with those proposed by Kleinheinz *et al.*[13]

In the γ-γ coincidence experiment we were able to establish the ground state rotational band definitely to spin 12, and tentatively

to 14. The 14 → 12 transition at 740 keV is seen as a very weak line in the 12 → 10 coincidence gate, and a γ-ray of this energy is definitely seen in singles. The excitation function data also appear to support the 14 → 12 assignment for this transition.[14] At 24 and 26 MeV, the 740-keV γ-ray could not be seen, but at 28 and 30 MeV, the line is clearly visible. Since this γ-ray was not seen in the (α,3n) experiments, the assignment as a transition from a high spin state in ^{182}W seems justified.

A plot of $2\mathcal{J}/\hbar^2$ vs. $\hbar^2\omega^2$ for the ^{182}W ground band is shown in Figure 7. The point associated with the tentative 14^{+} state deviates slightly from the line defined by the other members of the band, but ^{182}W is still an excellent rotor to spin 14.

The $I^{\pi} = 0^{+}$ member of the "β-band" was not seen in this work, and is taken from Kleinheinz *et al.*[13] Both β- and γ-band members decay via *E*2 transitions directly to the ground band.[6,7] The prominence of these interband transitions compared to intraband transitions is simply a result of the strong *E*2 energy dependence.

Plots of [E(I) - E(I-1)]/2I vs. $2I^2$ for most of the bands identified in ^{182}W are shown in Figure 8. For a perfect rotor, the points should form a straight line of zero slope. It is clear that the γ-band is highly perturbed, presumably from interactions with the β-band. In an attempt to account for the observed branching ratios and energy spacings in the β- and γ-bands, phenomenological three-band mixing calculations were carried out by Günther, *et al.*[15] using unperturbed ground-, β-, and γ-band states as a basis set. These

calculations do not account for the properties of the higher-lying states of the β and γ bands in our data. As we were interested in predicting the location of the 6^+ member of the γ band (for reasons to be discussed shortly), we repeated the three band mixing calculations using Günther's formalism, hoping to find a set of parameters which would more accurately reproduce the level energies.[14] However, we were unable to find any set of parameters which were able to fit the data accurately, indicating that the model space or the simple forms for the matrix elements used in Ref. 15 are incapable of realistically describing the interactions among those three bands. A similar conclusion was reached recently by Westerberg *et al.*[16]

There are several reasons why a simple β-γ-ground band mixing model may not describe the interaction of these three bands in ^{182}W. For example, it may be that interactions other than those assumed in Ref. 15 exist between these states. In fact, it is well known that low-lying 0^+ states in this region are not well-described as simple β-vibrations.[17] Excited 0^+ states can frequently have large intrinsic components.[18] Thus a thorough calculation would probably require more complex interactions. It is also possible that the failure of three-band-mixing to describe the collective states is due to an additional band, perhaps $K = 1$ in character, mixing with these states. As an example of how such mixing could

occur, RPA calculations done by Hamamoto (quoted in Ref. 13) indicate that roughly 25% of the γ band is made up of the $|K = 2, 3/2^-[512]\uparrow, 1/2^-[510]\uparrow\rangle$ state. This component can be Coriolis coupled directly with the $|K = 1, 3/2^-[512]\uparrow, 1/2^-[510]\uparrow\rangle$ and $|K = 1, 1/2^-[521]\uparrow, 1/2^-[510]\uparrow\rangle$ states, both of which have been tentatively assigned by Kleinheinz *et al.*[13] at approximately 2 MeV of excitation in ^{182}W.

In order to discuss the two-quasiparticle states in terms of the Nilsson model, it is necessary to know the nuclear shape in some detail. It is especially important to know the value of the hexadecapole deformation ε_4, since this parameter has a strong influence on the level ordering.[4] The magnitude of the hexadecapole deformation in ^{182}W and other nearby nuclei has been the subject of considerable debate. The ground-band hexadecapole *transition* moment in ^{182}W has been deduced by Bemis *et al.* from a Coulomb excitation measurement with alpha particles,[19] and their results indicate a value for ε_4 of 0.18 ± 0.06, significantly greater than the value of 0.06 predicted by Nilsson *et al.*[20] This value is also substantially larger than that obtained by Hendrie ($\varepsilon_4 \cong 0.08$) from nuclear inelastic scattering[21] on ^{182}W. In an attempt to determine which value of ε_4 is most consistent with nuclear spectroscopic data, Coriolis band fitting calculations were carried out for ^{181}W by Bernthal *et al.*[4] The results indicate it is possible to obtain reasonable fits to the ^{181}W even-parity states only by assuming values of ε_4 consistent with the predictions of Nilsson *et al.*[20] Therefore, our interpretation of the ^{182}W level structure relies upon the Nilsson states corresponding to deformations of $\varepsilon_2 = 0.24$ and $\varepsilon_4 = 0.06$ (see Figure 9).

The $K^\pi = 6^+$ two-quasi-proton band is rather unusual. The 6^+ assignment for the bandhead is taken from Galan *et al.*,[7] and the 214-keV transition from the 1971-keV state was found in that work to be *M*1, in agreement with the assigned band structure. The intrinsic structure of the band is believed to result from the singlet coupling of the $5/2^+[402]$ and $7/2^+[404]$ protons. The structure assignment is based on the observation that this band is seen in other even-even nuclei in this region.[22] From the diagram of Nilsson states shown in Figure 9, it can also be seen that there is no other way to form a low-lying $K^\pi = 6^+$ state.

Knowledge of the cascade-to-crossover ratios for γ-ray transitions within a band often makes it possible to distinguish between two-quasi-proton and two-quasi-neutron intrinsic particle structure of a band, provided one assumes that g_R and Q_0 for all the rotational bands is the same. The intrinsic quadrupole moment, Q_0, has been calculated from $B(E2)$ values obtained from ground band Coulomb excitation studies assuming[23]

$$Q_0 = [\frac{16\pi^2}{5} B(E2)]^{1/2}.$$

The value of Q_0 obtained in this way relates explicitly only to the ground band, but should apply reasonably well for the other rotational bands as well. The g_K values deduced experimentally from the observed branching ratios are compared with the theoretical value of g_K obtained from the Nilsson model, where in the asymtotic limit[22]

$$g_K = (1/K)[g_s + g_\ell(K-1)] \quad \text{for triplet states}$$
$$g_K = g_\ell \quad \text{for singlet states}$$

where g_s and g_ℓ are the intrinsic and orbital g-factors of the particle. In the case of the $K^\pi = 6^+$ band, the branching ratio could be determined for the spin 10 state at 2770.6 keV. The results are given in Table II. The theoretical value of g_K for a singlet two-quasi-proton state is 1, which agrees with the average experimental value of 0.99 ± 0.16. There is, however, evidence which might argue against this band being $K = 6$ in character, *viz.* the bandhead decays promptly to the $K = 0$ ground band. In ^{176}Hf, on the other hand, the $K^\pi = 6^+$ two-quasiparticle bandhead at 1333.1 keV decays with a half-life of almost 10 μs.[22] While *K* may not be a good quantum number for certain high-*j* orbitals in this region, the plot of $[E(I) - E(I-1)]/2I$ vs. $2I^2$ (Figure 8) gives little indication that this band is strongly mixed, as the points are nearly linear and the intercept (rotational constant) does not show the compression expected for a strongly Coriolis-mixed band (in contrast with the points associated with the $K^\pi = 4^-$, 5^-, or 6^- bands). Since there seems to be no reason to expect the $K^\pi = 6^+$ band to be strongly mixed, the *K*-forbidden γ-ray transitions out of the 1756.8-keV state would normally be highly hindered, and a measurable lifetime for the state is expected.

A possible explanation of the prompt decay from the $K^\pi = 6^+$ bandhead lies in a rather unusual mixing with the γ band, where the probable near-degeneracy of the two 6^+ states in ^{182}W may cause some mixing to occur. While the 6^+ member of the γ band was not seen experimentally, it is apparent from the level scheme that it must lie near the $K^\pi = 6^+$ bandhead. It was hoped that the three-band-mixing calculations discussed earlier would allow a reasonably accurate

estimate for the location of the 6^+ γ-band state. Though it was not possible to reproduce the known level energies, the various fits obtained indicated that the two 6^+ states are probably within 30 keV of each other, and could easily lie much closer.[14] Because of this near degeneracy, only a small interaction need be present to cause prompt decay of the $K^\pi = 6^+$ bandhead. Since the half-life of the γ bandhead is known from Coulomb excitation studies[25] to be roughly 0.3 ps, only about 0.01% γ-band admixture need be present in the $K = 6$ band to place the half-life below our experimental lower limit. The assignment of the 1756.8-keV band as being predominantly $K^\pi = 6^+$ is thus believed to be correct, and the short half-life of the $K^\pi = 6^+$ state is probably due to mixing with the 6^+ member of the γ band.

The remaining even-parity band seen in this study is that based on the isomeric state at 2230 keV. Nordhagen *et al.*[1] found this state to have a half-life of 1.4 μs and assigned it a spin and parity of $I^\pi = 9^+$ or 10^+. From the diagram of Nilsson States (Figure 9), it can be seen that a low-lying $K^\pi = 10^+$ state could be formed by a triplet coupling of the $9/2^-[514]$ and $11/2^-[505]$ protons or the $9/2^+[624]$ and $11/2^+[615]$ neutrons. On the other hand, low-lying 9^+ states are difficult to construct, so that the $K^\pi = 10^+$ assignment is preferred. Since either protons or neutrons may couple to form this state, it is desirable to identify the band members based on the two-quasiparticle state so that the branching ratios can be used to determine the intrinsic character of the state by evaluation of g_K. Because this state is isomeric, the γ rays associated with the intra-band transitions cannot be seen in prompt coincidence with the isomeric

or ground band transitions. By setting a gate off the prompt TAC peak, however, delayed coincidence spectra could be obtained. The prompt and delayed coincidence spectra associated with the $K^\pi = 10^+$ isomeric band are shown in Figure 10. The 262- and 283-keV γ rays are present in the 518-keV delayed spectrum, and prompt coincidence gates set on these γ rays allow the $K^\pi = 10^+$ band members to be identified with reasonable confidence to spin 14, and tentatively to spin 15. From the coincidence gate, it was possible to extract the branching ratio from the 3077.1-keV state. The theoretical values of g_K for triplet protons and neutrons are 1.25, and -0.23, respectively, assuming $g_s = 0.6\ g_s(\text{free})$. Table II shows that even if the observed intensity of the 586-keV transition were in error by 100%, the branching ratio would still indicate that this high-K band was predominantly a two-quasi-neutron band. Thus we characterize this band as predominantly the $|9/2^+[624\uparrow], 11/2^+[615\uparrow]>$ two-neutron state.

The measured half-life of 1.4 μs for the $K^\pi = 10^+$ isomer is actually much less than one might have expected. Using the Moszkowski single particle estimates, one finds that the decays are hindered by a factor of 5.2 per degree of K-forbiddenness. It is generally found experimentally that decays are hindered by a factor of 10 or 100 per degree of K-forbiddenness in deformed nuclei. The relatively small experimental retardation factor for the $K = 10$ bandhead implies that K is not strictly a good quantum number for the band; this is perhaps not surprising in view of its $i_{13/2}$ neutron character. It is, in fact, the only $i_{13/2}$ two-neutron isomer known in the deformed rare-earth region, and the $i_{13/2}$ neutron orbitals are known to be strongly

Coriolis-mixed in odd-A nuclei. From the plot of $[E(I) - E(I-1)]/2I$ vs. $2I^2$ for the band (Figure 8), it is seen that the band-member spacings are somewhat compressed relative to the nearly pure $K^\pi = 6^+$ and $K^\pi = 7^-$ proton bands, but are rather similar to the $K^\pi = 8^-$ neutron band. Some compression can be understood in terms of Coriolis coupling with high-lying bands containing $i_{13/2}$ particles.

The *yrast* structure of ^{182}W is of special interest, first because of its striking contrast with the ^{180}W *yrast* behavior (Figure 7), and secondly because the $K = 10^+$ two-neutron configuration apparently becomes *yrast* in ^{182}W above spin 16. We have summarized the salient aspects of the *yrast* behavior of the neutron rich tungsten isotopes 177-182 in an earlier letter,[26] where we argue that *both* $i_{13/2}$ neutrons and $h_{9/2}$ protons[3] may be involved in producing the ^{180}W *yrast* band anomaly. In the case of ^{182}W, an examination of the behavior of the $i_{13/2}$ band structure in neighboring ^{181}W leads us to expect that backbending in ^{182}W should not occur from decoupling of $i_{13/2}$ neutrons. In the Stephens and Simon model,[27] the presence near the Fermi surface of $i_{13/2}$ neutrons with predominatly low-Ω components is most likely to produce backbending in the *yrast* band of an even-even nucleus. A straightforward calculation shows that the $i_{13/2}$ neutron remains quite strongly coupled to the core in ^{181}W, even at relatively high spins. This situation is in contrast to that in ^{179}W where a large hexadecapole deformation and the location of the Fermi surface apparently conspire to produce a relatively decoupled $i_{13/2}$ structure.[26] In ^{181}W and ^{182}W, however, the Fermi surface has emerged into the large gap expected at $N = 108$ in the neutron spectrum,[20] and the situation evidently is substantially changed. Indeed,

the valence $9/2^+[624]$ and $11/2^+[615]$ neutrons in ^{182}W are found to produce the observed 1.4-μsec $K^\pi = 10^+$ isomer, and the associated band structure is characteristic of strong particle-core coupling. The appearance of this isomer at 2231 keV suggests that other seniority-two, $\nu i_{13/2}$ configurations must lie still higher in the spectrum. Thus, backbending in ^{182}W cannot occur in the usual spin range (14-18$\hbar$) from intersection of the ground band with a decoupled $\nu i_{13/2}$ 2-quasiparticle structure. This conclusion seems entirely consistent with the data of Figure 7.

It is also noteworthy that the isomeric $|9/2^+[624]; 11/2^+[615]\rangle$ band apparently forms the *yrast* sequence above spin 16. Figure 11 shows a plot of E vs. I(I+1) for the ground and $K = 10^+$ bands, and it is evident that the two should cross near spin 16. It would be most interesting to examine the behavior of these two bands near and above this crossing point. If the spin-16 states are in fact nearly degenerate, one could hope to extract matrix elements for mixing between the two bands at that spin if interband γ-ray transitions were observed. One also notes that the triplet $K^\pi = 10^+$ 2-neutron band should evolve into a decoupled $i_{13/2}$ structure at some appreciably higher spin.

These high-spin features could be explored in a reaction which transfers more angular momentum into the product nucleus. The ^{182}Hf$(\alpha,4n)^{182}$W reaction would be ideal but it requires a target of ^{182}Hf ($t_{1/2} = 9 \times 10^6$ y), in principle obtainable from double neutron capture on ^{180}Hf. An alternative method now available would be the Coulomb excitation of ^{182}W with heavy-ion beams, but the interband transitions may be relatively weak and difficult to see in such an experiment.

B. Odd Parity Bands

The $K^{\pi} = 2^{-}$ band was identified to spin 4 in the transfer reaction work of Kleinheinz *et al.*,[13] and much evidence has accumulated indicating that the band is based on an octupole vibration.[13,15,29] In β-decay studies,[6] the band was established to spin 6, and in-beam it is seen to spin 11 (see Figure 12). The higher band assignments are based on the energy spacings of the levels and the observed decrease of the cascade-to-crossover γ-ray intensity ratio as angular momentum increases, a result of the energy dependence of the *E*2 transition probability. The excitation function and angular distribution results are in reasonable agreement for the transitions up to the spin 9 state; these data were not reliable for the weakly populated higher-spin states.

Figure 13 shows a plot of $\frac{[E(I) - E(I-1)]}{2I}$ vs. $2I^2$ for the octupole band, and indicates that the band is strongly perturbed; the points form two branches with the odd spin members depressed. These odd-even shifts arise from second order Coriolis mixing with the $K^{\pi} = 0^{-}$ octupole band via the $K^{\pi} = 1^{-}$ octupole band.[30] Only odd-spin members of the $K = 0$ band are expected to lie low in energy, so that only the odd-spin members of the $K = 2$ band are expected to be significantly mixed. As the locations of the $K = 0$ and $K = 1$ octupole bands are not known, an experimental estimate of the interaction matrix elements cannot be made, although theoretical matrix elements and bandhead energies have been calculated by Neergård and Vogel.[31] Several papers exist in the literature dealing with the properties of the octupole band,[15,29] but the calculations were carried out in those papers under the assumption that no $K = 0$ or $K = 1$ admixture

is present in the $K = 2$ octupole band. The large perturbations shown by the $[E(I) - E(I-1)]/2I$ vs. $2I^2$ plot place this assumption in question.

Note that the upper branch of the octupole band plot shows a marked deviation from smooth behavior for the point representing the energy difference between the $I = 6$ and $I = 5$ states. This anomalous point is the result of mixing with the $K^{\pi} = 4^{-}$ band. Because the $I = 5$ and $I = 6$ states of the $K = 4$ band both lie between the $I = 5$ and $I = 6$ states of the octupole band, the octupole states tend to be pushed apart. In contrast, the corresponding states in the $K = 4$ band are pushed together, as can be seen on the plot for this band (Figure 8). Strong mixing of the $K = 4$ band with the octupole band is also implied by the fact that the $K = 4$ states decay primarily to the octupole states rather than via intraband cascades.

The $K^{\pi} = 4^{-}$, 5^{-}, and 6^{-} bands were all seen in the (d,t) and (τ,α) reaction work of Kleinheinz *et al.*,[13] and the Nilsson assignments shown in Figure 12 are taken from that work. The highest state in the $K = 5$ band and the highest two states in the $K = 6$ band were seen only in this work and are assigned to these bands largely on the basis of energy spacings and decay patterns. In addition, the assignments for the $K = 6$ band are consistent with the angular distribution and excitation function measurements. The transfer reaction studies indicated that these three bands were strongly mixed, and the interband transition strength seen here supports this conclusion.

The remaining two odd parity bands are given tentative Nilsson and spin assignments on the basis of somewhat meager evidence. The bandhead at 1978 keV (Figure 12) is known to be $I^{\pi} = 6^{-}$ or 7^{-} from

decay studies.[6,7] The intense 18-keV decay to the $I^{\pi}K = 7^{-}6$ state at 1960 keV (Figure 12) suggests that these two states are highly mixed, lending support to the $K^{\pi} = 7^{-}$ assignment for the 1978-keV state. As the $|9/2^{-}[514\uparrow], 5/2^{+}[402\uparrow]>$ two-quasi-proton state is expected to lie quite low in the spectrum, this assignment is preferred, although other reasonably low-lying neutron and proton $I^{\pi} = 7^{-}$ two-quasiparticle states can be formed. It seems probable, however, that the band is based on a two-quasi-proton state, since the 1978-keV state decays via a strong 221-keV γ ray to the $K^{\pi} = 6^{+}$ two-quasi-proton bandhead. Since these bands are of different parity, no mixing can occur between them. If the $K^{\pi} = 7^{-}$ band were a two-quasi-neutron structure, decay to the $K^{\pi} = 6^{+}$ bandhead should be quite hindered compared to decays to other two-quasi-neutron states. Again, the members of this band are assigned primarily on the basis of energy spacings and decay patterns. The angular distributions and excitation function measurements were in most cases inconclusive in verifying the assignments.

We should also note that the conclusions of the preceding discussion imply mixing between the 1978- and 1960-keV states, an example of neutron-proton configuration mixing. If this is the case, the mixing primarily results from the accidental near-degeneracy of the two states, as the states do not satisfy the conditions usually required for significant p-n configuration mixing.[32] The empirical rule that significant configuration mixing occurs only when the unpaired particles occupy orbitals on both sides of the Fermi surface can be understood by looking at the form of the off-diagonal matrix

element for the residual n-p interaction, V_{np}. Massman *et al.*[32] show that

$$<\psi_{n_1n_2}|V_{np}|\psi_{p_1p_2}> = |(u_{n_1}v_{n_2}u_{p_1}v_{p_2} + v_{n_1}u_{n_2}v_{p_1}u_{p_2})$$

$$<n_1\bar{p}_2|V_{np}|n_2p_1> - (u_{n_1}v_{n_2}v_{p_1}u_{p_2} +$$

$$v_{n_1}u_{n_2}u_{p_1}v_{p_2})<n_1\bar{p}_1|V_{np}|\bar{n}_2p_2>|$$

where $|\psi_{n_1n_2}>$ is the two quasi-neutron excited state and u and v are the usual pair occupation amplitudes. In the pairing factors of the above equation, only the combination uv occurs. Because u is large for orbitals above and v for orbitals below the Fermi surface, the product, and thus the off-diagonal matrix element, is largest when the orbitals of interest straddle the Fermi surface. In the case of the 1960- and 1978-keV states in ^{182}W, it can be seen from the Nilsson diagram of Figure 9 that neutron-proton mixing between low-lying components of the same K would violate this condition. The nearly degenerate energies of these two states apparently still causes appreciable mixing, despite the unfavorable location of the Fermi surface.

The remaining band seen in this work is tentatively assigned as $K^{\pi} = 8^{-}$. Assignments for the states in this band are in agreement with the angular distribution data, but excitation function data are inconclusive. An interesting characteristic of this band is the sudden appearance of a strong interband transition from the 2328-keV

state. This branching can be understood if the 2120.2-keV state were $I^{\pi} = 8^{-}$ and if it were mixed with the $I^{\pi} = 8^{-}$ state of the $K^{\pi} = 6^{-}$ band at 2114.1 keV. Since the perturbed energies are only 6 keV apart, an interaction matrix element of only 3 keV (in the approximation of two-band mixing) would account for the splitting if the states were initially degenerate, and Coriolis interactions could easily account for a matrix element of this magnitude. Finally, from the Nilsson states shown in Figure 9, one would expect the $K^{\pi} = 8^{-}$ band to lie slightly below the $K^{\pi} = 10^{+}$ isomeric band, as this band does. On the basis of these arguments, the band is tentatively assigned to be a two-quasi-neutron band formed by the triplet coupling of the $9/2^{+}[624]$ and $7/2^{-}[503]$ neutrons.

4. SUMMARY AND CONCLUSIONS

As a result of the large number of low-lying high-Ω single-particle states in ^{182}W, the in-beam γ-ray investigation produced considerable new information for high-lying members of an unusually large number of rotational bands. The apparent success of the Nilsson model in predicting the observed two-quasiparticle states for the deformation parameters $\varepsilon_2 = 0.24$ and $\varepsilon_4 = 0.06$ indicates that the spectroscopic data are consistent with the nuclear deformations predicted by Nilsson, and argues strongly that the deformed shell model gives quite an accurate description of intrinsic nuclear structure in this region of the nuclear chart.

In view of the continuing interest in backbending, the experimental identification of a $K^{\pi} = 10^{+}$, $|9/2^{+}[624\uparrow]; 11/2^{+}[615\uparrow]>$ two-quasi-neutron band makes it of interest to examine higher spin states in ^{182}W. The $K = 10$ band should become the *yrast* structure above spin 16 in ^{182}W, but the two $i_{13/2}$ neutrons are unlikely to be sufficiently decoupled from the core rotation at the crossing point to produce backbending behavior in the *yrast* band in the usual sense. Backbending in the g.r.b. above the crossing between the $K^{\pi} = 10^{+}$ band and the ground band would therefore require the decoupling of lower-Ω (but higher energy) $i_{13/2}$ neutron orbits, or perhaps a similar decoupling of $h_{9/2}$ protons.[3] Either heavy-ion Coulomb excitation of ^{182}W, or the ^{182}Hf(α,4nγ) reaction could yield new data on this possibility. It would also be of interest to determine whether a similar situation exists in ^{184}Os, an isotone of ^{182}W. This nucleus displays sharp backbending in the ground band,[2] and it is conceivable that an intruding decoupled $i_{13/2}$ neutron structure of the Stephens-Simon type is

responsible for this behavior. No $K^{\pi} = 10^{+}$ isomer has been reported in ^{184}Os.

We conclude that there is strong circumstantial evidence[26] for involvement of $i_{13/2}$ neutrons both in backbending-type behavior in ^{180}W and in the sudden disappearance of that behavior in ^{182}W. In view of the equally compelling data of the Jülich group[3] that seem to implicate $h_{9/2}$ protons in the ^{182}Os *yrast* behavior, it seems quite possible that both $i_{13/2}$ neutrons and $h_{9/2}$ protons may play a part in backbending phenomena in this region.

APPENDIX. The Decay of ^{182m}Re to ^{182}W

The decay of ^{182m}Re was investigated primarily because the in-beam γ-ray spectroscopy study indicated that errors existed in the current decay schemes.[6,7] The principal tool used in this study was the two-parameter γ-γ coincidence technique, but the high-resolution singles spectrum shown in Fig. 14 was also taken so that γ-ray energies and intensities in the complex low-energy region of the spectrum could be measured accurately.

The ^{182m}Re activity was produced by bombarding 1-mil natural tantalum foil with 41-MeV alpha particles from the MSU cyclotron. The source was allowed to cool for four days to eliminate 13 h ^{182g}Re. Coincidence data were taken at 90° geometry with detectors of 18% and 10% efficiency. Table III lists the γ-rays placed in the ^{182m}Re decay scheme, which is shown in Figure 15. A few coincidence gates associated with ^{182m}Re decay are shown in Fig. 16. Figure 16a shows the 226.2-keV gate, and it is seen that the 221.6-keV γ-ray is the most prominent line in the spectrum, indicating that the 226.2-keV γ-ray is a transition to the 1978.4-keV level. The presence in this spectrum of γ-rays associated with the 1960.3-keV level requires the existence of the intense 18-keV transition from the 1978.4-keV level seen by Harmatz *et al.*[9] Figures 16b and 16c show the spectra associated with gates set on the high- and low-energy portions of the 300-keV doublet. The similarity of the gated spectra strongly suggests the doublet of states at 1960.3 and 1960.7 keV. The 151.2-keV γ-ray could be placed only on the basis of the energy of the transition, and the

131.4-keV transition from the 1960.7-keV state assigned by Harmatz *et al.*[9] was not seen. Figure 16d shows the 214.3-keV gated transition and shows clearly the γ-rays associated with the 1756.8-keV level. The coincidence evidence for the 2335-keV and 2120.5-keV states is weak. However, these levels are firmly established from the in-beam study.

The intensities of γ rays only in a range from 84 keV to 360 keV were measured in this brief study. The intensities of the higher energy γ-rays were taken from Galan *et al.*[7] Conversion electron intensities needed to calculate β-decay feedings were obtained when possible from the conversion coefficients quoted by Galan *et al.*[7] or Ö. Nilsson *et al.*[33] In the region below 84 keV, the conversion electron data of Harmatz *et al.*[7] were used. When no experimental conversion coefficients existed, β-decay feedings were deduced from theoretical conversion coefficient values taken from Hager and Seltzer[34] and Dragoun *et al.*[35] Log*ft* values were calculated with use of the tables of Gove and Martin.[36]

In summary, the ^{182m}Re decay study resulted in placement of new levels at 1917.0, 1971.1, 2114.4, 2204.5, and 2335.4 keV in ^{182}W. States assigned at 1500.3, 1632.8, 1734.8, and 1983.2 keV in previous investigations have been deleted. The γ-ray branching ratios and log*ft* values are largely unchanged.

The spin and parity assignments given in the decay scheme are discussed in detail in the text of this paper, though it should be mentioned that the assignment of the $K^{\pi} = 6^{+}$ bandhead at 1756.8 keV as a high-K state (rather than as the spin-6 member of the γ band)

is in agreement with the large EC-β^{+} feeding (12%) from the $K^{\pi} = (7^{+})$ parent. Information from this decay study, especially regarding the low-energy transitions and EC-β^{+} feedings, was essential to construction of the final ^{182}W level scheme from the in-beam $(\alpha,2n\gamma)$ experiments.

References

1) R. Nordhagen, R. M. Diamond, and F. S. Stephens, Nucl. Phys. A138 (1971) 231.

2) R. A. Warner, F. M. Bernthal, J. S. Boyno, and T. L. Khoo, Phys. Rev. Lett. 31 (1973) 34.

3) A. Neskakis, R. M. Lieder, M. Müller-Veggian, H. Beuscher, W. F. Davidson, and C. Mayer-Böricke, Nucl. Phys. A261 (1976) 189.

4) F. M. Bernthal, B. D. Jeltema, J. S. Boyno, T. L. Khoo, and R. A. Warner, Phys. Rev. Lett. 33 (1974) 915.

5) R. F. Casten, Phys. Lett. 49B (1974) 161.

6) J. J. Sapyta, E. G. Funk, and J. W. Mihelich, Nucl. Phys. A139 (1970) 161.

7) P. Galan and M. Vejs, Czech. J. Phys. B22 (1972) 18.

8) G. Sletten and P. Knudsen, Nucl. Instr. Meth. 102 (1972) 459.

9) B. Harmatz, T. H. Handley, and J. W. Mihelich, Phys. Rev. 123 (1961) 1758.

10) V. A. Ageev, V. I. Gavriljuk, T. Kupryashkin, G. D. Latyshev, I. N. Ljutyj, Yu. V. Makoveckij, and A. I. Feoktistov, An. SSSR. ser. fiz. 34 (1970) 2135.

11) Th. Lindblad, H. Ryde, and P. Kleinheinz, Nucl. Phys. A210 (1973) 253.

12) S. A. Hjorth, H. Ryde, and B. Skånberg, Arkiv för Fysik 38 (1968) 537.

13) P. Kleinheinz, P. J. Daly, and R. F. Casten, Nucl. Phys. A208 (1973) 93.

14) B. D. Jeltema, M.S. Thesis, Michigan State University (1974).

15) C. Günther, P. Kleinheinz, R. F. Casten, and B. Elbeck, Nucl. Phys. A172 (1971) 273.

16) L. Westerberg, L. O. Edvardson, and G. Ch. Madueme, Nucl. Phys. A255 (1975) 427.

17) J. D. Immele and G. L. Struble, Lawrence Livermore Laboratory preprint UCRL-77519 (1975) and private communication.

18) F. M. Bernthal, J. O. Rasmussen, and J. M. Hollander, Phys. Rev. C 3 (1971) 1294.

19) C. E. Bemis, P. H. Stelson, F. K. McGowan, W. T. Milner, J. L. C. Ford, Jr., R. L. Robinson, and W. Tuttle, Phys. Rev. C 8 (1973) 1934.

20) S. G. Nilsson *et al.*, Nucl. Phys. A131 (1969) 1.

21) D. L. Hendrie, Phys. Rev. Lett. 31 (1973) 478.

22) T. L. Khoo, J. C. Waddington, and M. W. Johns, Can. J. Phys. 51 (1973) 2307; T. L. Khoo *et al.*, Phys. Rev. Lett. 28 (1972) 1717.

23) P. H. Stelson and L. Grodzins, Nucl. Data A1, No. 1 (1965) 21.

24) P. Gilad, G. Goldring, R. Herber, and R. Kalish, Nucl. Phys. A91 (1967) 633.

25) D. G. Alchazov *et al.*, ZhETF (USSR) 35 (1958) 1325; Izv. Akad. Nauk SSSR (ser. fiz.) 28 (1964) 229.

26) F. M. Bernthal, C. L. Dors, B. D. Jeltema, T. L. Khoo, and R. A. Warner, Phys. Lett. 64B (1976) 147.

27) F. S. Stephens and R. S. Simon, Nucl. Phys. A183 (1972) 257.

28) F. M. Bernthal, J. S. Boyno, T. L. Khoo, and R. A. Warner, Phys. Rev. Lett. 33 (1974) 1313.

29) P. Herzog, M. J. Canty, and K. D. Killig, Nucl. Phys. A187 (1972) 49.

30) T. L. Khoo, J. C. Waddington, Z. Preibisz, and M. W. Johns, Nucl. Phys. A202 (1973) 289.

31) K. Neergård and P. Vogel, Nucl. Phys. A145 (1970) 33.

32) H. Massmann, J. O. Rasmussen, T. E. Ward, P. E. Haustein, and F. M. Bernthal, Phys. Rev. C 9, (1974) 2312.

33) Ö. Nilsson, S. Högberg, S. E. Karlsson, and G. M. El-Sayad, Nucl. Phys. A100 (1967) 351.

34) R. S. Hager and E. C. Seltzer, Nucl. Data A4 (1968) Nos. 1 and 2.

35) O. Dragoun, H. C. Pauli, and F. Schmutzler, Max Planck Institute Report No. MPIH-1968-V14, 1968 (unpublished).

36) N. B. Gove and M. J. Martin, Nucl. Data A10 (1971) No. 3.

Table 1. γ-Rays Observed in the $^{180}Hf(\alpha,2n)^{182}W$ Reaction at 26 MeV

E_γ (keV)[a]	I_γ[b]	Assignment	Multipolarity[c]	γ-Ray Anisotropy (A_2/A_0)
84.7	38 (3)	1373.8 → 1289.2	*M*1 + *E*2	0.15 (4)
100.1	350 (30)	100.1 → 0	*E*2	0.05 (3)
107.0 (2)	11.9 (0.)	1660.4 → 1553.2	*M*1 + *E*2	
108.4 (2)	40 (3)	1769.0 → 1660.4	*M*1	
111.1 (3)	4 (2)	1621.3 → 1510.2		
113.5	106 (9)	1487.5 → 1373.8	*M*1 + *E*2	-0.41 (1)
116.4 (2)	5.4 (0.4)	1373.8 → 1257.4		
130.8	31 (3)	1960.3 → 1829.5	*M*1 + *E*2	-0.72 (3)
133.8	41 (3)	1621.3 → 1487.5	*E*2 + *M*1	0.21 (11)
145.4 (2)	23 (5)	1769.0 → 1623.5	*M*1	-0.30 (15)
147.8	25 (5)	1769.0 → 1621.3		
148.9 (2)	7 (4)	1978.4 → 1829.5		
150.2	11 (2)	(1660.4 → 1510.2)		
152.4	100 (10)	1373.8 → 1221.4	*E*1	-0.19 (3)
154.1	11 (2)	2114.4 → 1960.3		-0.97 (16)
156.4	87 (7)	1487.5 → 1331.1	*E*1	-0.12 (5)
160.2	12 (1)	2120.5 → 1960.3		-0.95 (11)
169.2	40 (3)	1829.5 → 1660.4	*M*1	-0.11 (5)
172.9	30 (3)	1660.4 → 1487.5	*M*1	
178.5	35 (3)	1621.3 → 1442.8	*E*1	-0.20 (8)
179.4	19.2 (1.5)	1553.2 → 1373.8	*E*2 + *M*1	0.23 (8)
186.7 (2)	5.6 (0.8)	(1810.9 → 1623.5)		-0.8 (6)
189.6	12 (1)	1810.9 → 1621.3		
191.4	29 (2)	1960.3 → 1769.0	*M*1	-0.25 (1)
198.4	53 (4)	1487.5 → 1289.2	*E*2	
203.6	16.2 (1.3)	1960.3 → 1756.8	*E*2	
206.1 (2)	4.6 (0.7)	1829.5 → 1623.5		
207.7	13.2 (1.1)	2328.0 → 2120.5		-0.77 (20)

Table 1 (Continued)

209.9 (2)	5.0 (0.5)	(1978.4 → 1769.0)	(*M*1)	0.7 (5)
213.6 (2)	17.0 (3.0)	2328.0 → 2144.4		-0.5 (3)
214.4	54 (4)	1971.1 → 1756.8	*M*1	
215.4	33 (3)	1769.0 → 1553.2	*E*2	
217.5	20.3 (1.6)	1660.4 → 1442.8	*E*1	-0.32 (10)
221.2 (2)	15.0 (1.5)	1978.4 → 1756.8	*E*1	
222.0	64 (6)	1553.2 → 1331.1	*E*1	
226.2	61 (6)	2204.5 → 1978.4	*M*1	
229.3	1000[b]	329.4 → 100.1	*E*2	0.26 (6)
236.1	21.2 (2.1)	2564.1 → 2328.0		
241.7	25.7 (2.1)	2212.8 → 1971.1		0.10 (4)
247.5	79 (6)	1621.3 → 1373.8	*E*2	0.33 (9)
251.3	58 (5)	2455.8 → 2204.5		
256.6	56 (4)	1809.7 → 1553.2	*M*1	
260.2	12.0 (1.0)	2824.3 → 2564.1		-1.12 (3)
262.3	46 (4)	2492.9 → 2230.6		-0.81 (4)
264.0	25.6 (2.0)	1553.2 → 1289.2	*E*2	0.25 (9)
267.4	8.3 (0.9)	2480.2 → 2212.8		
275.3 (2)	13.4 (1.3)	2731.1 → 2455.8		-1.1 (7)
276.4	19.0 (2.0)	1829.5 → 1553.2	*E*2	
279.8 (3)	11.7 (2.3)	3104.1 → 2824.3		0.4 (3)
281.5	51 (4)	1769.0 → 1487.5	*E*2	0.24 (16)
283.0	16.0 (2.0)	2775.9 → 2492.9		-0.8 (3)
286.6	22.0 (3.0)	1660.4 → 1373.8	*E*2	0.33 (17)
290.4 (2)	15.0 (3.0)	2770.6 → 2480.2		
295.9	25.0 (2.0)	1917.0 → 1621.3		0.38 (13)
298.8	12.0 (3.0)	3029.9 → 2731.1		0.36 (15)
299.8 (2)	19.0 (2.0)	1960.3 → 1660.4		
302 (1)	13 (5)	3077.1 → 2775.9		-0.22 (14)
313.6 (3)	4 (1)	1756.8 → 1442.8		
318.7	56 (5)	2087.7 → 1769.0		0.51 (7)

Table 1 (Continued)

320.2 (2)	11.0 (2.0)	3397.3 → 3077.1		
323.4	55 (5)	1810.9 → 1487.5	*E*2	0.41 (13)
337 (1)	3 (2)	3734 → 3397.3		
339.1	27.8 (2.2)	1960.3 → 1621.3	*E*2	0.43 (6)
341.6	17.2 (1.4)	1829.5 → 1487.5	*E*2	
345.4	22.4 (2.3)	2114.4 → 1769.0		0.52 (9)
351.1	800 (60)	680.5 → 329.4	*E*2	0.28 (7)
355.9 (2)	32 (6)	2334.3 → 1978.4		
357.0 (2)	56 (8)	2274.0 → 1917.0		0.44 (19)
362.4 (3)	13.0 (1.5)	2131.4 → 1769.0		
372.5	27.4 (2.2)	1993.8 → 1621.3		0.30 (12)
399.8	56 (5)	2487.5 → 2087.7		0.50 (17)
406.8 (2)	13.2 (5.0)	2323.8 → 1917.0		
414.6	26.6 (2.1)	2225.5 → 1810.9		0.16 (8)
437.2	27.6 (2.2)	2711.2 → 2274.0		
452.3	21.2 (1.7)	2446.1 → 1993.8		0.5 (4)
464.0	480 (40)	1144.5 → 680.5		0.29 (9)
514.1 (3)	12 (3)	2739.6 → 2225.5		
518.5	63 (5)	2230.6 → 1712.1		
534.5	9.7 (0.9)	2980.6 → 2446.1		
558.2 (4)	8.5 (1.7)	2770.6 → 2212.8		0.5 (4)
567.6	222 (18)	1712.1 → 1144.5		0.27 (9)
586.2	21.3 (1.7)	3077.1 → 2492.9		0.35 (24)
660.6	49 (4)	2372.7 → 1712.1		
740.1 (2)	6.5 (0.7)	3112.8 → 2372.7		
927.6 (2)	17.7 (1.8)	1257.4 → 329.4	*E*2	
943.3 (4)	8.9 (1.8)	(1623.5 → 680.5)		
1001.8	35 (3)	1331.1 → 329.4	*E*2	
1076.4	60 (5)	1756.8 → 680.5		
1086.5	73 (6)	2230.6 → 1144.5		
1113.5	56 (5)	1442.8 → 329.4		

Table 1 (Continued)

1121.4	245	(20)	1221.4 →	100.1	*E2*
1157.7 (4)	23.3	(1.9)	1257.4 →	100.1	*E0* + (*M1*) + *E2*
1180.5 (4)	32	(3)	1510.2 →	329.4	
1189.1 (2)	103	(8)	1289.2 →	100.1	*E1* + *M2* + *E3*
1221.8 (4)	166	(13)	1221.4 →	0	*E2*
1230.9 (2)	139	(11)	1331.1 →	100.1	
1257.2 (4)	34	(3)	1257.4 →	0	*E2*
1273.9 (4)	29	(5)	1373.8 →	100.1	
1293.9 (4)	51	(4)	1623.5 →	329.4	
1342.3 (2)	52	(4)	1442.8 →	100.1	*E2*
1410.9 (5)	7.7	(1.6)	1510.2 →	100.1	
1426.8 (5)	51	(5)	1756.8 →	329.4	
1454.3 (5)	17.5	(1.9)	(1553.2 →	100.1)	

[a] Error is 0.1 keV unless otherwise indicated.

[b] Normalized to the 229.3-keV γ-ray. Errors in parentheses.

[c] Taken from Ref. 7.

Table 2. g_K values from branching ratios for $K^\pi = 6^+$ and $K^\pi = 10^+$ bands in ^{182}W

$I^\pi K$	Transition	Energy (keV)	*E2/M1* Branching Ratio	$\lvert g_K - g_R \rvert / Q_0$ [a]	g_K
10+6	10 → 8	558.2	0.57±0.3 [b]	0.11 ±0.03	0.96±0.19
	10 → 9	290.4			-0.46±0.19
10+6	10 → 8	558.2	0.48±0.3 [c]	0.12 ±0.04	1.02±0.26
	10 → 9	290.4			0.53±0.26
13+10	13 → 11	586.0	0.2 ±0.1 [d]	0.081±0.020	-0.27±0.13 [e]
	13 → 10	302.0			

[a] Q_0 is taken from reference 23 and g_R is from reference 24.

[b] Branching ratio raken from γ-ray singles data. Large error results from uncertainty in resolving the weak doublet at 557 keV.

[c] Value taken from the 241.6-keV coincidence gate. Large uncertainty results from angular correlation effects and uncertainty in the detector relative efficiency in the coincidence arrangement.

[d] This value could be obtained only from coincidence data (262.3-keV gate) as the 586-keV γ-ray is believed to be the smaller component of an unresolved doublet.

[e] For 100% error in *E2/M1* branching ratio, the error in g_K = ±0.26. The sign of δ and hence of $(g_K - g_R)$ are determined to be negative from angular distribution data for the $11^+ \rightarrow 10^+$ and $12^+ \rightarrow 11^+$ transitions in the $K^\pi = 10^+$ band.

Table 3. γ-Rays Observed in Decay of ^{182m}Re to Levels in ^{182}W

Energy[a]	γ-Ray Intensity[b]	Energy[a]	γ-Ray Intensity[b]
18.1	-	160.2	9.3 (0.6)
19.9	-	169.15	440 (30)
31.7	34 (16)	172.87	139 (9)
39.1	12 (3)	178.47	88 (5)
42.7	11 (1)	179.40	117 (7)
60.7	4 (2)	187.34	12.5 (1.2)
65.8	106 (10)	188.54	5.1 (0.5)
67.9	880 (60)	189.65	15 (7)
84.68	107 (7)	191.39	260 (20)
100.10	580 (40)	198.34	157 (13)
107.13	55 (4)	203.55	19 (2)
108.58	31 (2)	206.00	20 (2)
110.38	4 (4)	208.26	24 (2)
111.07	8.1 (0.6)	209.40	19 (2)
113.68	189 (12)	214.32	43 (3)
116.23	20 (2)	215.73	30 (2)
130.81	290 (20)	217.55	127 (8)
133.80	93 (6)	221.61	250 (20)
145.43	26 (2)	222.07	330 (30)
147.69	35 (3)	226.19	119 (8)
148.86	68 (5)	229.32	1000[a]
149.45	35 (3)	247.46	196 (13)
150.25	20 (2)	256.45	370 (30)
151.15	17 (2)	264.07	139 (9)
152.43	330 (20)	276.31	340 (20)
154.10	9 (3)	281.45	221 (15)
156.39	280 (20)	286.56	274 (18)

Table 3 (Continued)

295.67 (0.1)	8 (3)	1180.8 (0.3)	21.5 (1.0)
299.90 (0.1)	49 (10)	1189.0 (0.1)	351 (10)
300.36 (0.1)	66 (15)	1221.4 (0.1)	677 (14)
313.98 (0.1)	31 (2)	1231.0 (0.1)	579 (11)
323.40 (0.1)	68 (5)	1257.5 (0.1)	41.4 (1.2)
339.06 (0.1)	216 (14)	1273.8 (0.1)	36.7 (1.7)
342.03 (0.1)	41 (3)	1279.8 (0.3)	2.4 (0.3)
345.46 (0.1)	19 (2)	1289.2 (0.1)	29.4 (0.6)
351.07 (0.1)	400 (30)	1291.8 (0.4)	9.1 (0.9)
357.04 (0.1)	21 (2)	1294.0 (0.3)	62.7 (1.2)
891.9 (0.1)	1.3 (0.2)	1330.9 (0.2)	14.6 (1.3)
928.0 (0.1)	14.4 (1.5)	1342.7 (0.1)	100 (25)
943.2 (0.3)	8.8 (1.4)	1373.8 (0.1)	11.5 (0.4)
959.7 (0.1)	7.8 (1.5)	1387.4 (0.1)	10.3 (1.0)
1001.7 (0.1)	95.7 (3.4)	1410.1 (0.1)	10.8 (0.7)
1044.4 (0.1)	11.1 (0.4)	1427.3 (0.2)	381 (7)
1076.2 (0.2)	410 (12)	1439.3 (0.3)	6.2 (0.4)
1088.5 (0.3)	7.7 (0.8)	1453.1 (0.1)	1.5 (0.3)
1113.3 (0.1)	183 (4)	1521.3 (0.4)	3.7 (0.4)
1121.3 (0.1)	855 (25)	1560.4 (0.4)	2.8 (0.3)
1157.3 (0.1)		1631.4 (0.5)	0.49 (0.09)
1158.1 (0.1)	48.7 (1.2)		

[a] Unless otherwise indicated, error may be taken as ±0.05 keV.

[b] Normalized to the 229.3-keV γ-ray. Only γ-ray energies and intensities in the region from 84 keV to 360 keV were measured in this study. Energies and intensities below 84 keV are taken from Ref. 9 and those above 360 keV are taken from Ref. 7.

Figure Captions

1. The γ-ray singles spectrum from the $^{180}Hf(\alpha,2n\gamma)^{182}W$ reaction at E_α = 26 MeV.
2. High-resolution γ-ray singles spectrum from the $^{180}Hf(\alpha,2n\gamma)^{182}W$ reaction at E_α = 26 MeV.
3. A partial level scheme for states ranging from ground to 2230.6 keV in ^{182}W. All known transitions are shown. Dots are below those transitions placed on the basis of coincidence data obtained in this study. Asterisks (*) behind γ-ray energies indicate that the transition is known only from decay studies.[9,6] The level at 1137 keV is taken from Kleinheinz *et al.*[13]
4. A partial level scheme for states ranging from 1487.5 keV to 3734 keV in ^{182}W. All known transitions are shown. See Figure 3 for significance of dots and asterisks.
5. The band structure assigned for states deduced in ^{182}W. The symbols π and ν indicate whether proton or neutron single particle orbitals form the dominant configuration. Dotted levels indicate that the band assignment is tentative, and energies in parentheses indicate that the level is tentative.
6. The even-parity bands observed in ^{182}W. Only the two most intense transitions associated with each level are shown. Refer to Figure 5 for level energies.
7. "Backbending" type plot for ^{182}W ground rotational band. The ^{180}W data of Ref. 26 are shown for comparison.
8. $\Delta E[I \rightarrow I-1]/2I$ vs. $2I^2$ for rotational bands in ^{182}W.

9. The diagram of Nilsson states for ^{182}W assuming deformation parameters of ε_2 = 0.24 and ε_4 = 0.06. The Fermi surface is placed arbitrarily just above the orbitals known to form the ground state in neighboring odd-*A* nuclei. Level energies not corrected for pairing.
10. Prompt and delayed γ-ray coincidences associated with the $K^\pi = 10^+$ isomeric band: 518.5-keV prompt spectrum (top); 518.5-keV delayed spectrum (middle); 262.3-keV prompt spectrum (bottom).
11. A plot of energy vs. I(I+1) for the ground and $K^\pi = 10^+$ bands in ^{182}W.
12. The odd parity band structure observed in ^{182}W. Only the two most intense transitions associated with each level are shown. Refer to Figure 5 for level energies.
13. $[E(I) - E(I-1)]/2I$ plotted vs. $2I^2$ for the $K^\pi = 2^-$ octupole bands in ^{182}W.
14. The high-resolution γ-ray singles spectrum associated with the decay of 64 h ^{182m}Re.
15. Levels of ^{182}W populated in the decay of 64 h ^{182m}Re.
16. Selected coincidence gates associated with ^{182m}Re decay.

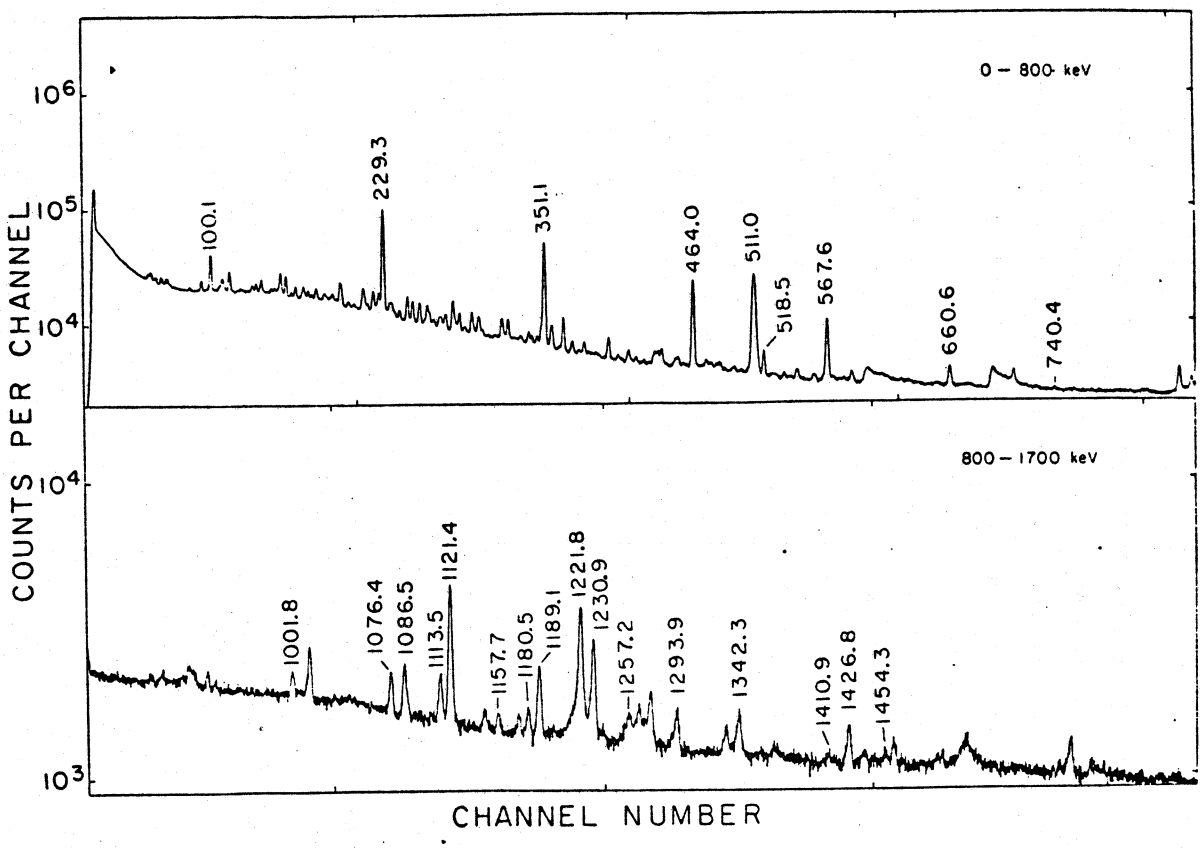

Figure 1

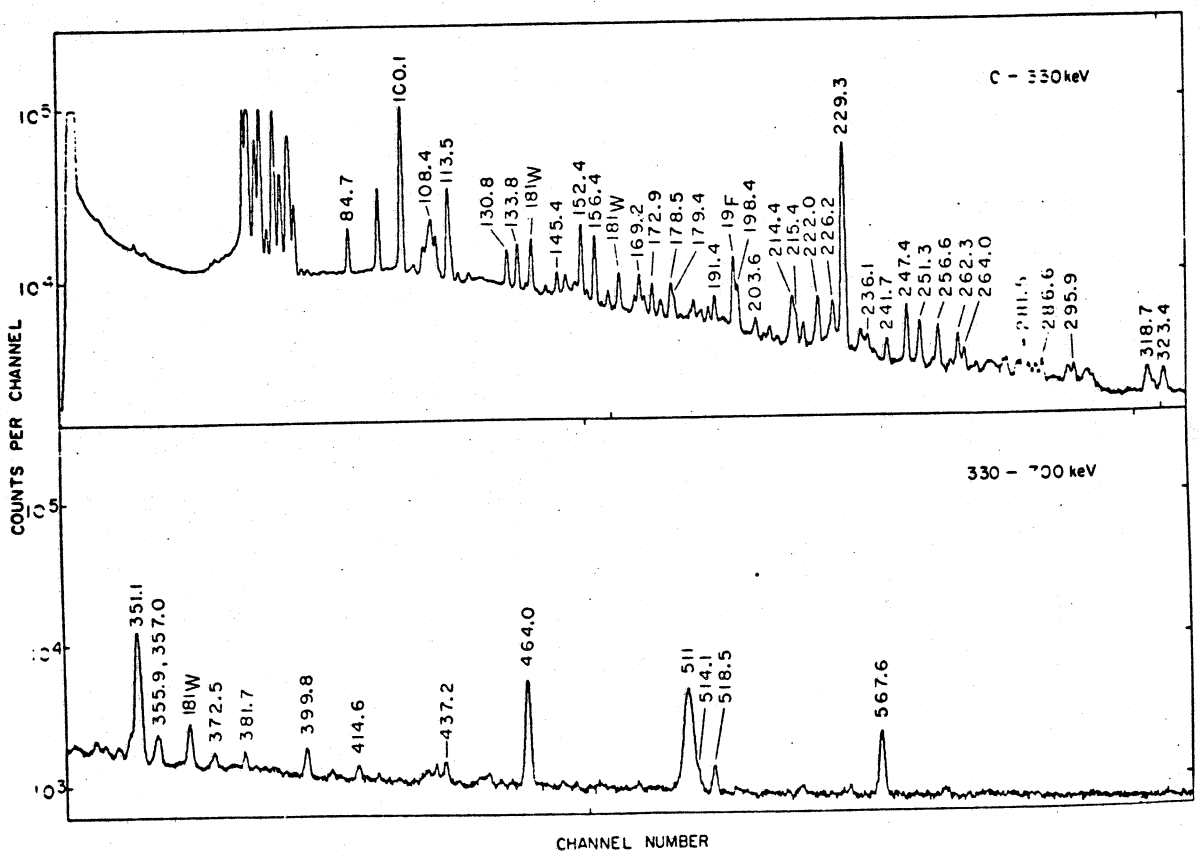

Figure 2

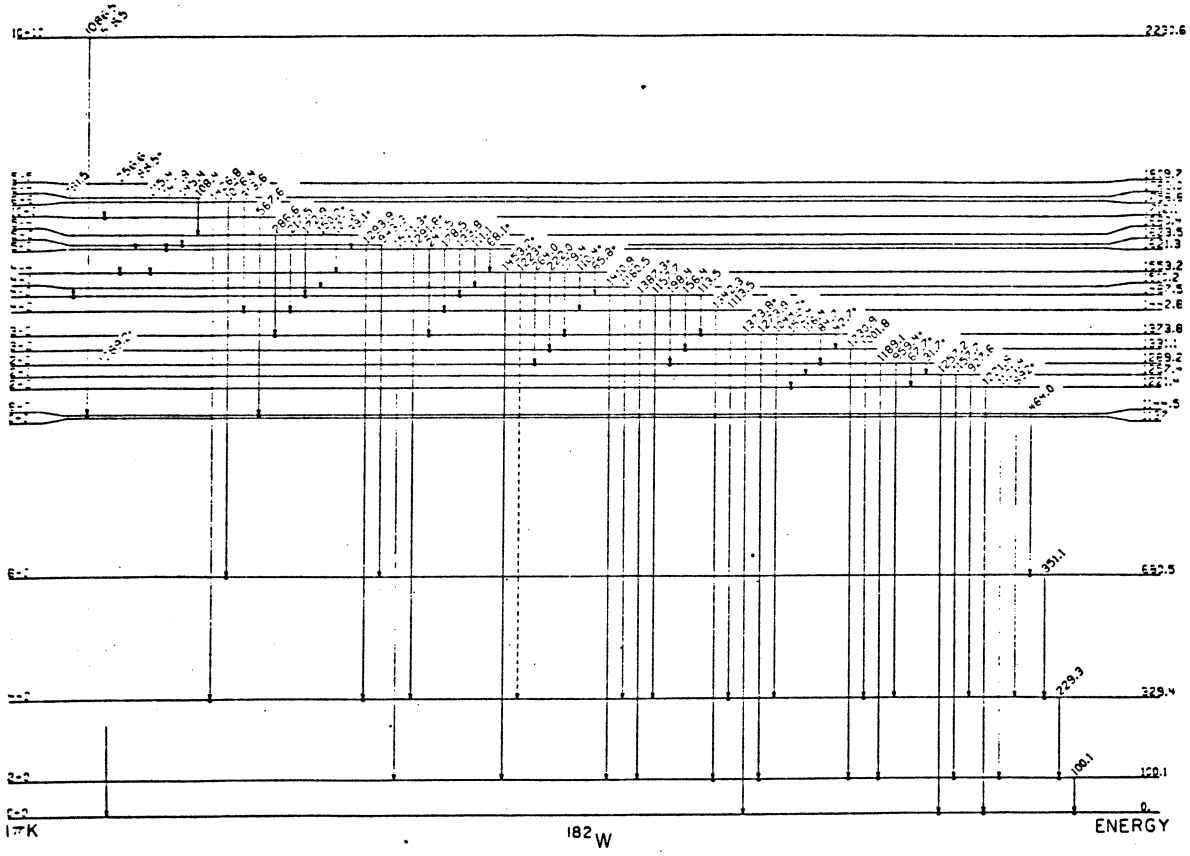

Figure 3

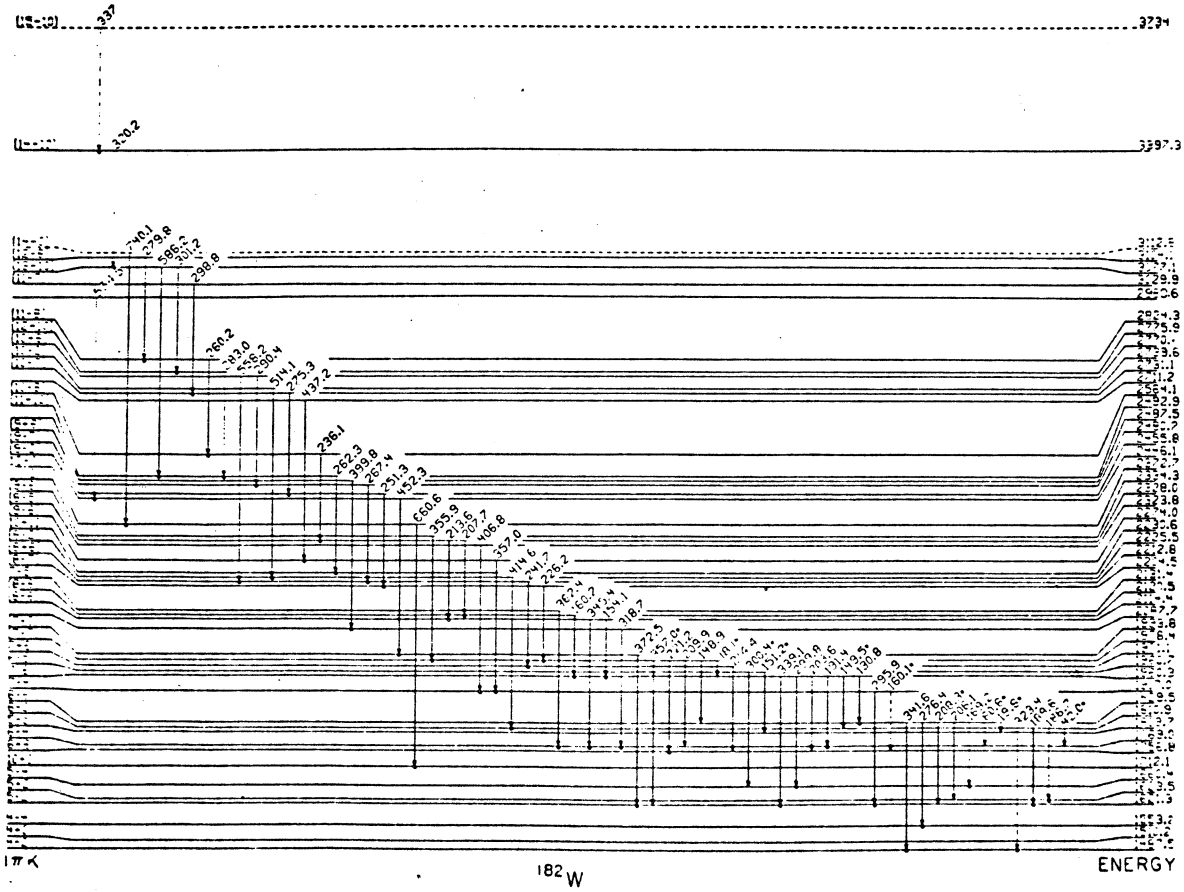

Figure 4

ROTATIONAL BANDS IN ^{182}W

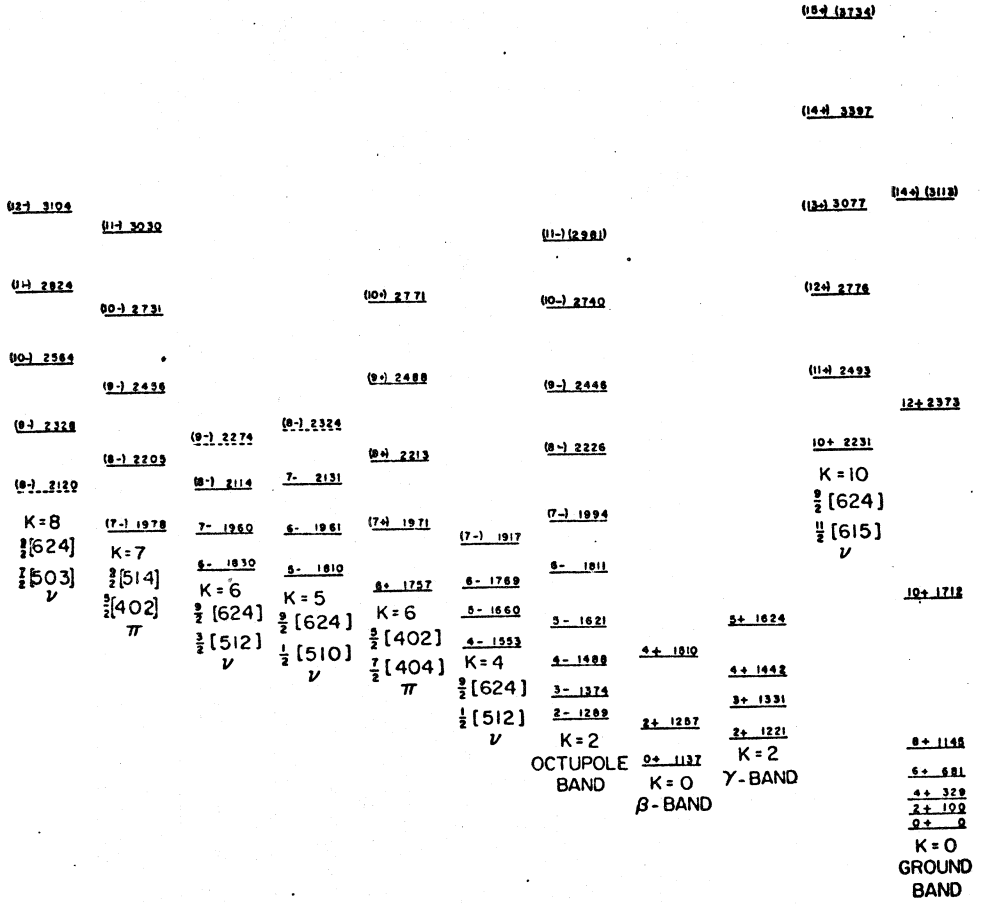

Figure 5

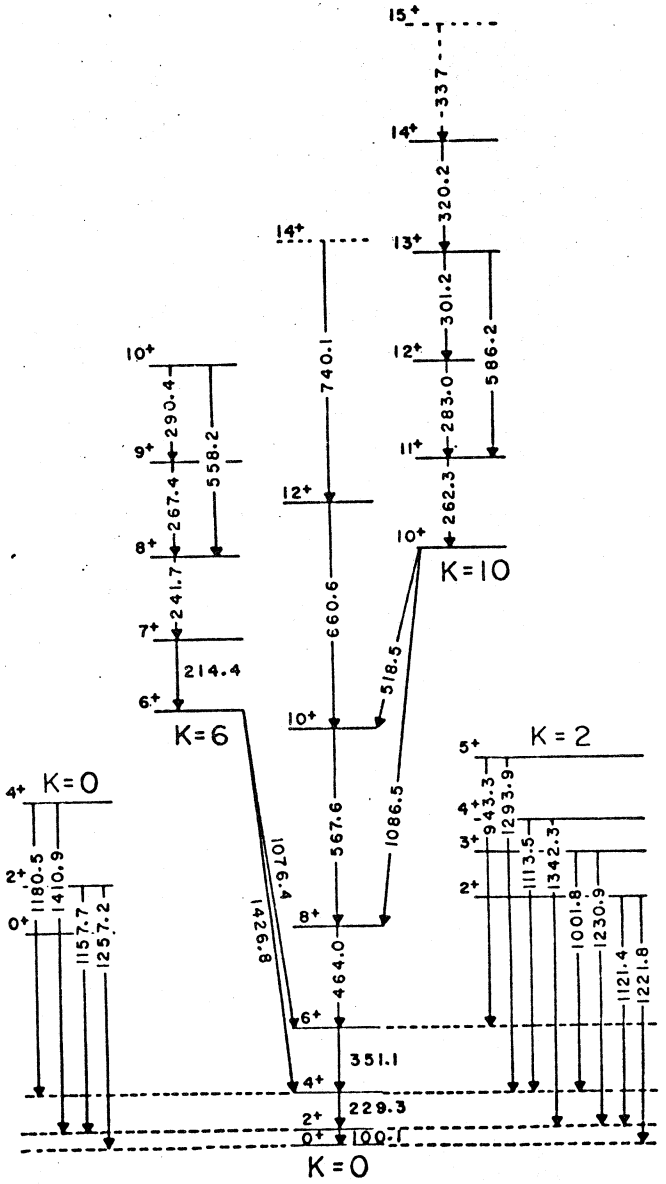

Figure 6

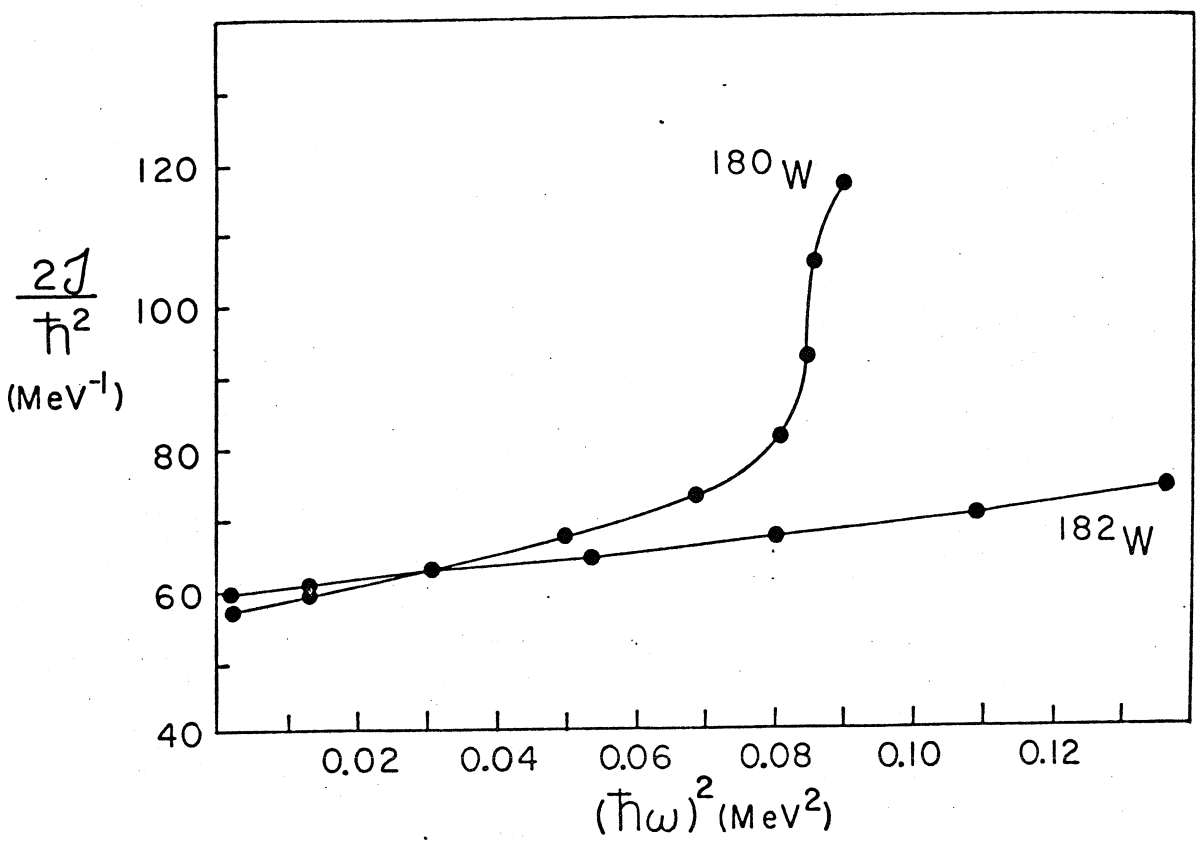

Figure 7

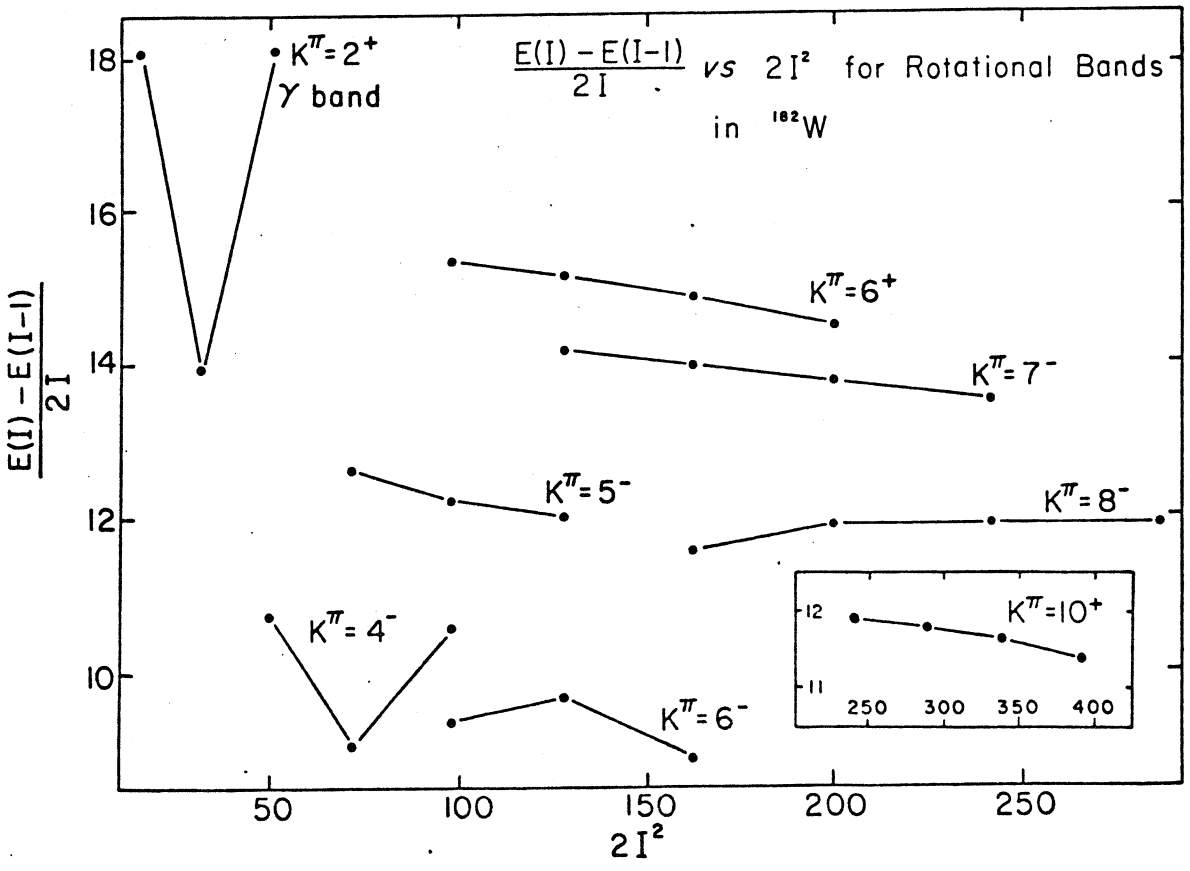

Figure 8

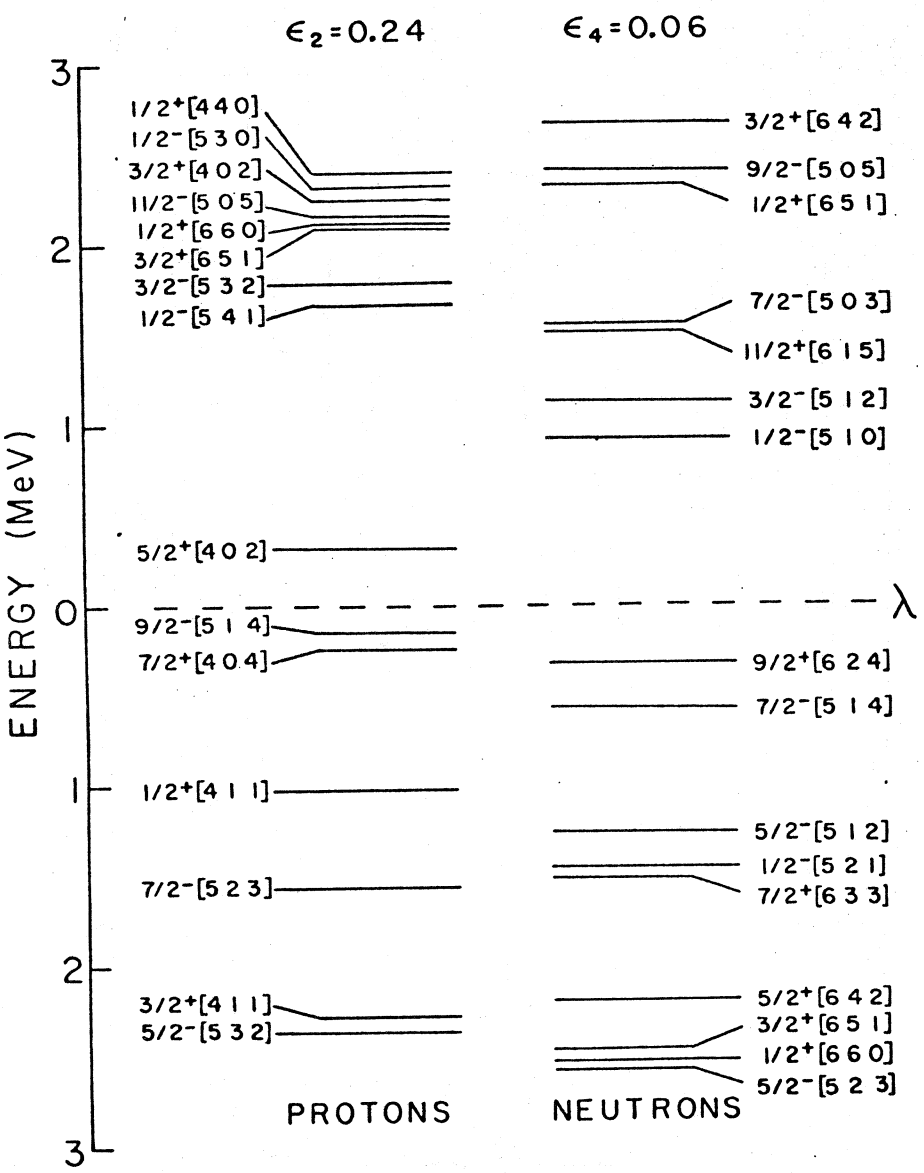

Figure 9

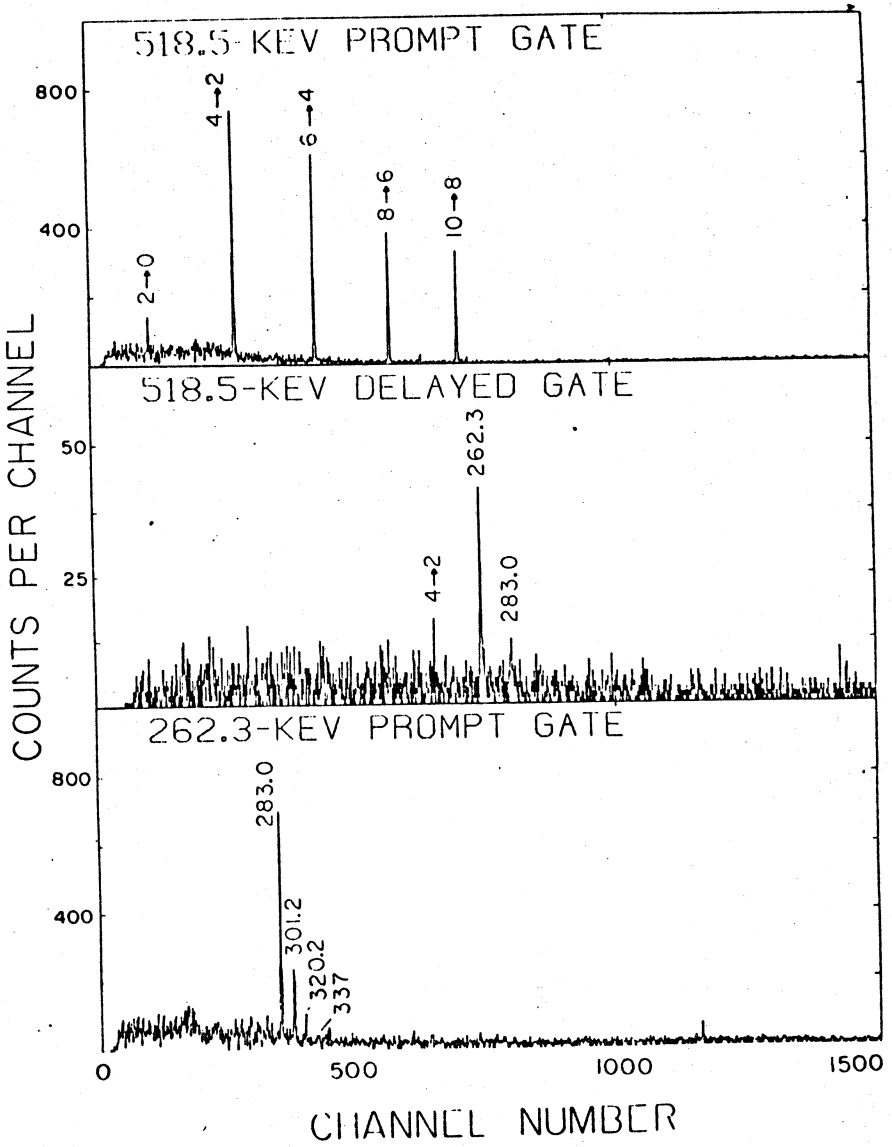

Figure 10

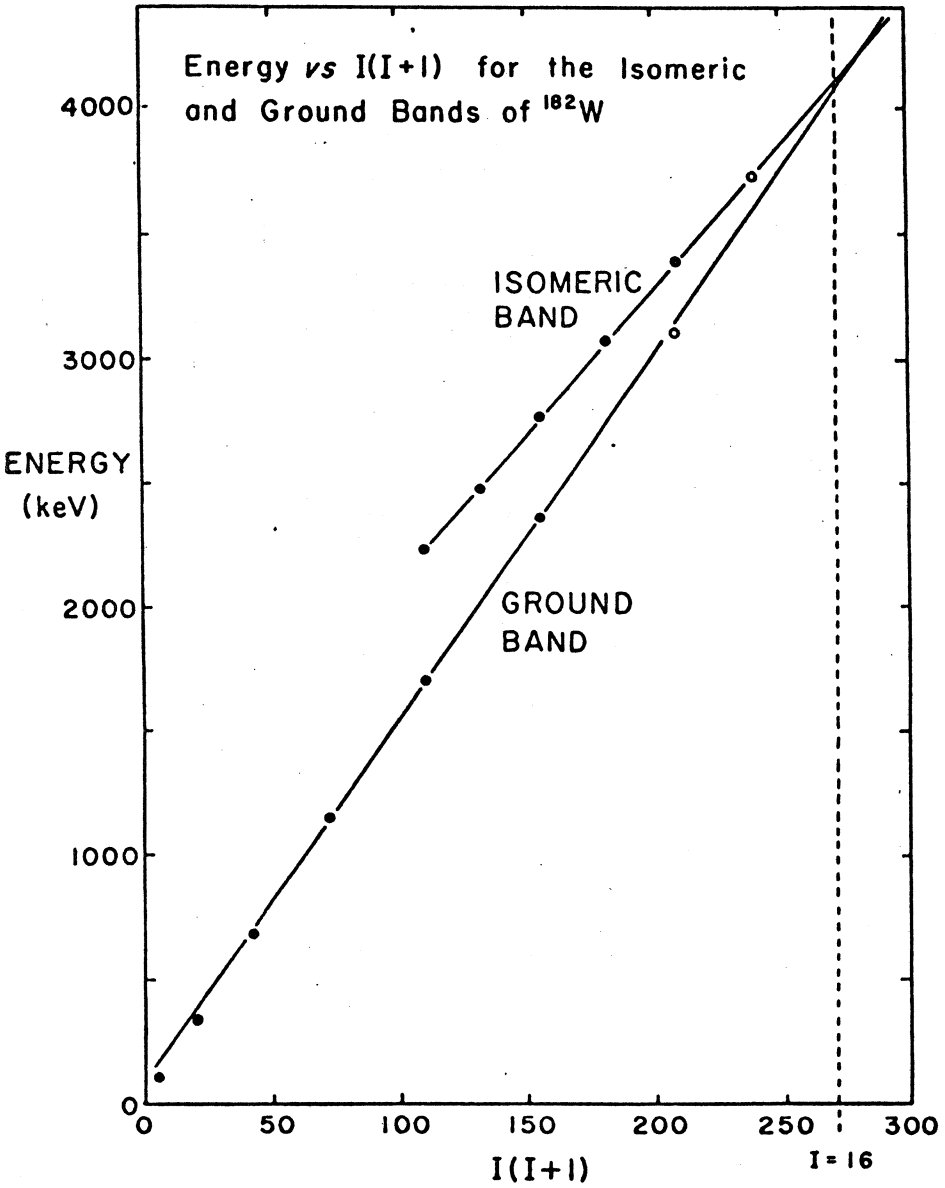

Figure 11

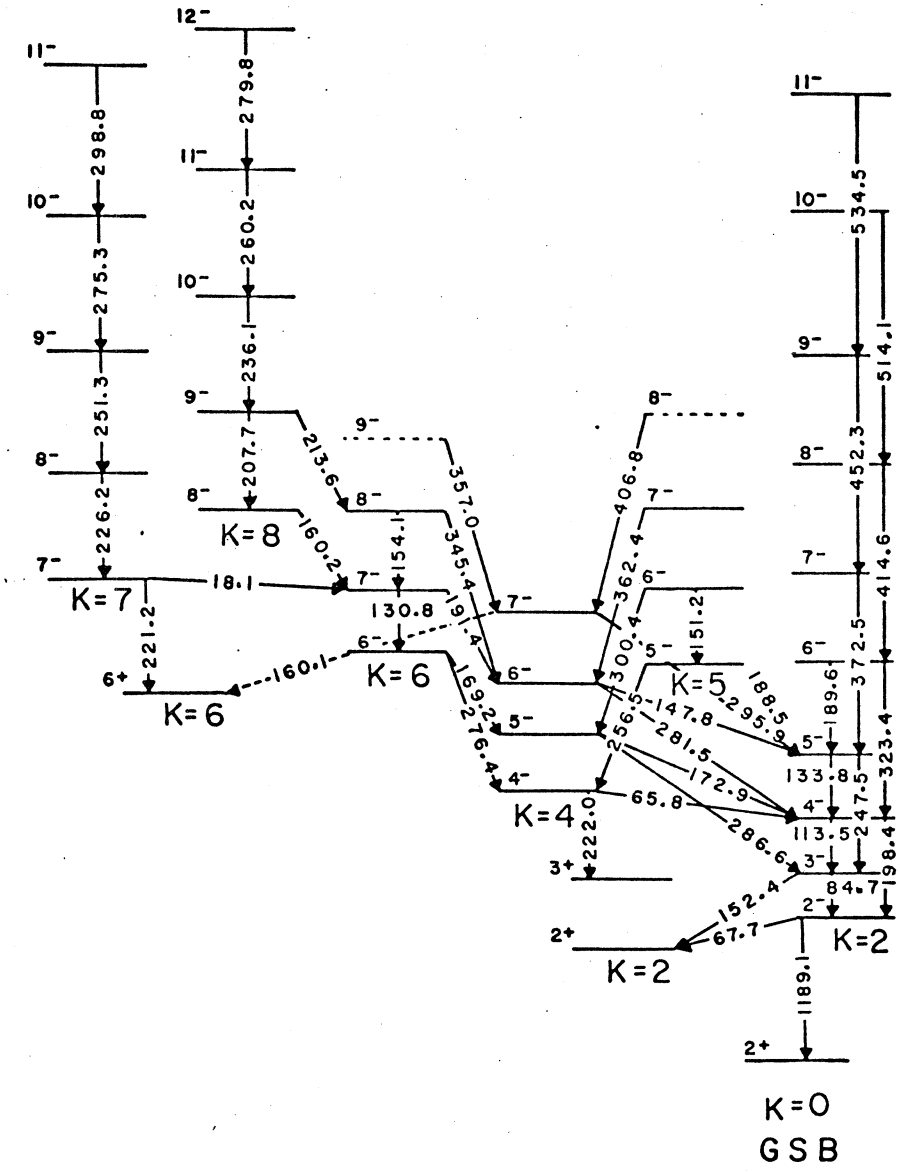

Figure 12

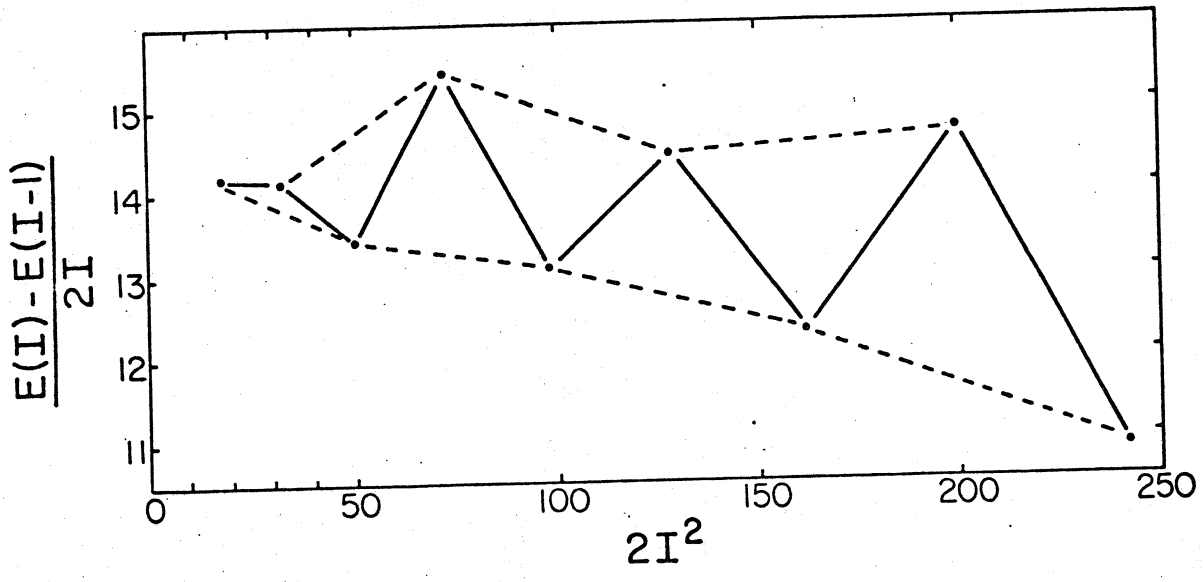

Figure 13

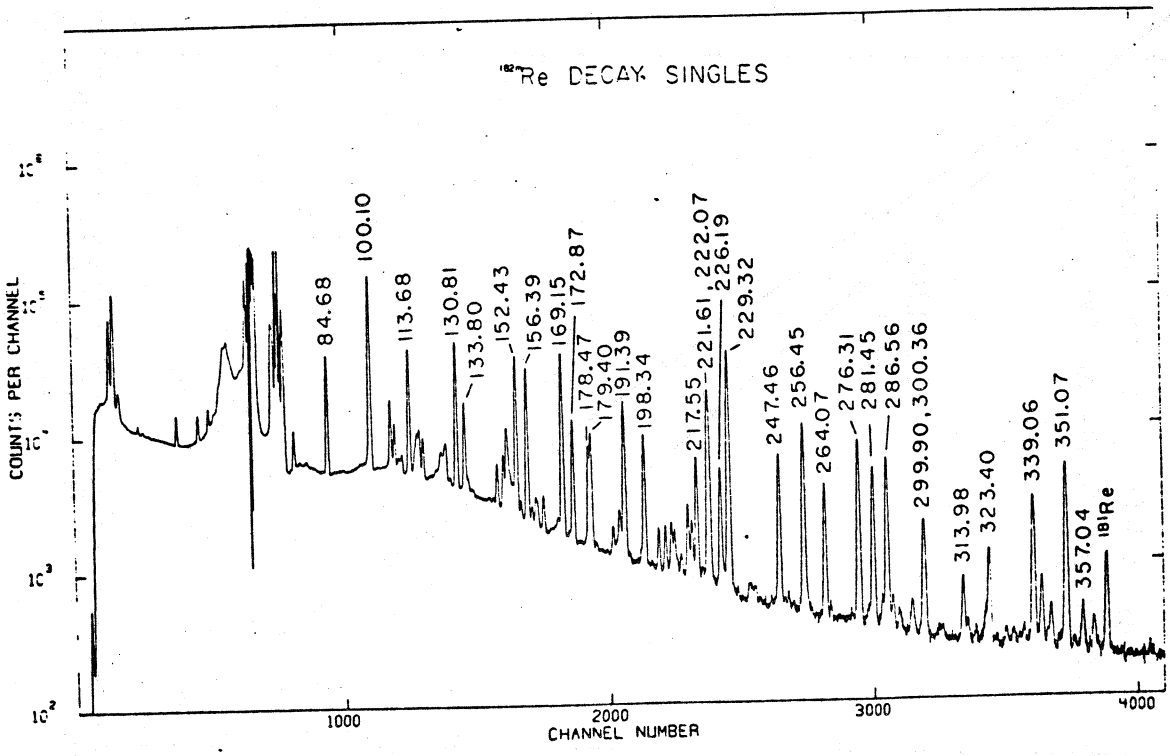

Figure 14

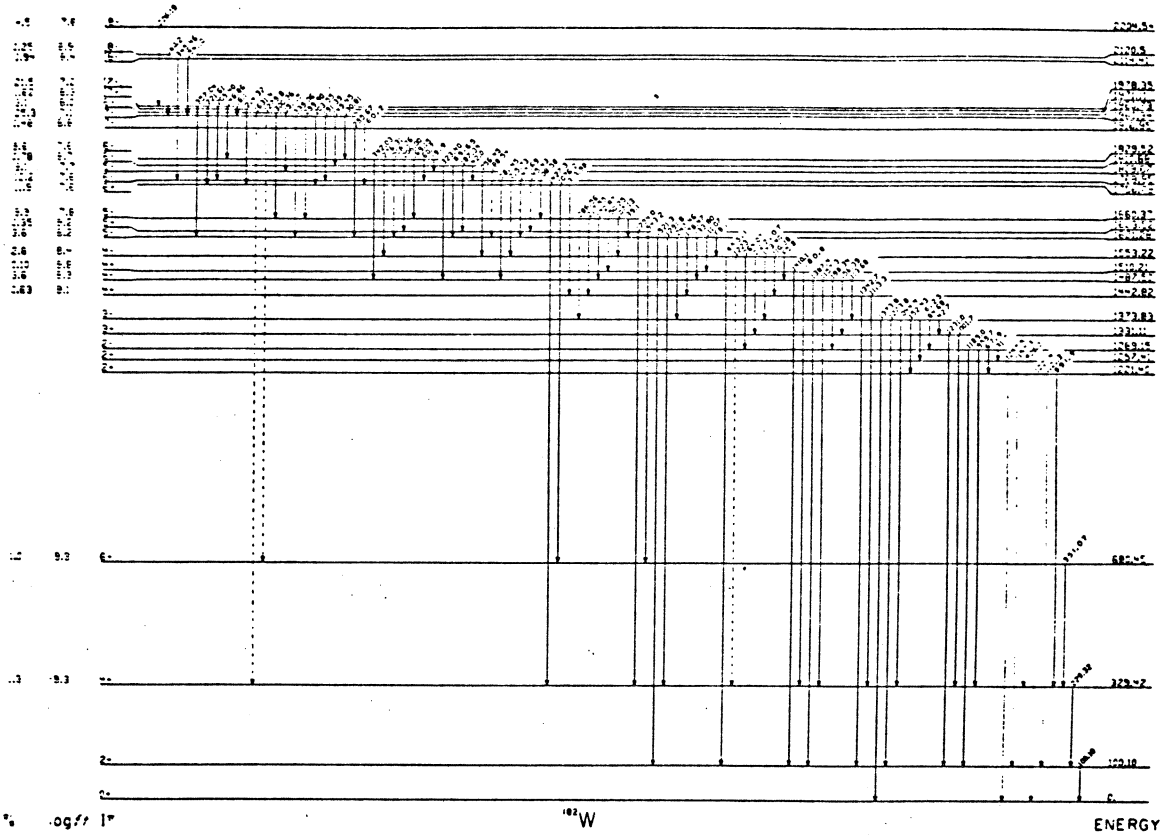
^{182}W
ENERGY

Figure 15

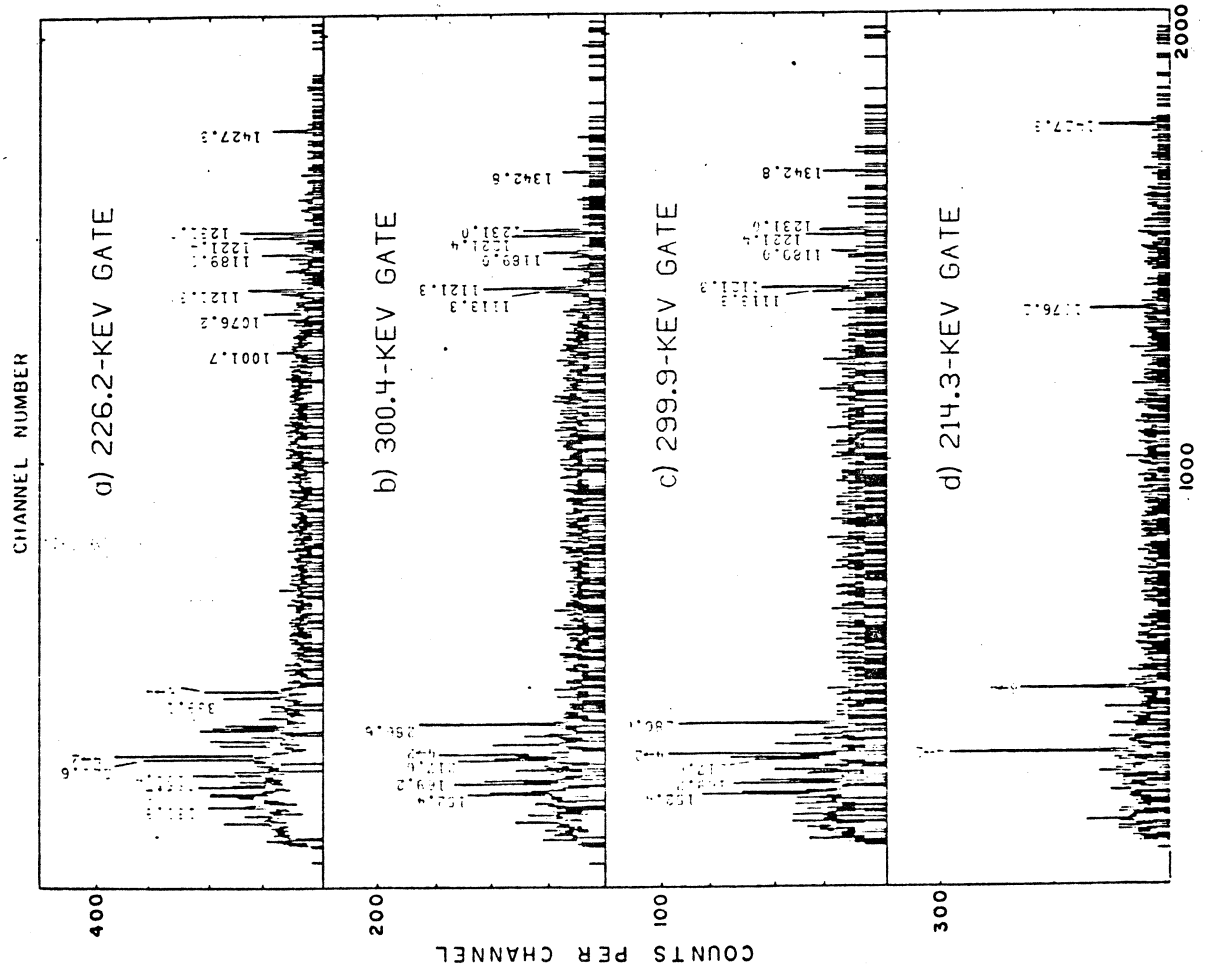
a) 226.2-KEV GATE
b) 300.4-KEV GATE
c) 299.9-KEV GATE
d) 214.3-KEV GATE
CHANNEL NUMBER
COUNTS PER CHANNEL
400
200
100
300
1000
2000